Uplift, denudation, and their causes and constraints over geological timescales

Kerry Gallagher

Uplift, denudation, and their causes and constraints over geological timescales

Kerry Gallagher

Dept. of Earth Sciences and Engineering

Imperial College London

London, SW7 2AS

England

ABSTRACT

We define uplift and denudation, then review the basic principles underlying the mechanisms for producing uplift, and the methodologies used to quantify the geological timescale denudation history of uplifted regions. Uplift is represents work done against gravity, and does not necessarily lead immediately to rapid denudation. The causes of uplift can be categorised according to the principal driving mechanism – stress, thermal or gravitational factor, although all three can operate to varying degrees. Simple formulations and examples. are presented to demonstrate the magnitude of uplift in various situations. The magnitude of denudation over geological timescales is quantified through various methods, which are sensitive to depth, pressure or temperature. These include cosmogenic surface exposure dating, thermochronology (apatite fission track analysis, (U-Th)/He dating), porosity-depth relationship (overcompaction), and by comparing predicted subsidence to the observed subsidence history.

INTRODUCTION

In this chapter, we review some of the mechanisms and methods relevant to understanding uplift and/or denudation. Here we use the phrase "and/or" to indicate that one may occur without the other. The Earth Science literature has many examples where the phrase "uplift and denudation", or more commonly "uplift and erosion" are used almost as one word. Clearly, an uplifted region may undergo denudation, although the absolute elevation of a given region is not necessarily the dominant control on denudation. The Tibetan Plateau, for example, is at a present day elevation of about 5.5 km, but not apparently undergoing rapid denudation. Similarly, changes in the rate denudation may occur in response to changes in drainage, which may reflect geomorphological processes, such as river capture, rather than being intimately linked with the timing of uplift.

Firstly, we describe some of the terminology used in the context of uplift/denudation, and then consider some of the causes of uplift, focussing on the first order physical controls. We also provide an overview of the methods used to quantify denudation and denudation chronologies on geological timescales. Finally, we briefly consider some approaches used to model regional denudation on large scales, and how these are linked to tectonics. We focus on the basic principles, but do not review in detail the many applications of these methods, preferring to cite comprehensive review papers and representative case studies, where appropriate

SOME DEFINITIONS

One consequence of denudation is the removal of any direct evidence of uplift, and the problem is then one of inferring denudation, and linking this to uplift. This is not a straightforward procedure, and typically relies on assumptions regarding cause and effect. Over the years, the terms uplift and denudation (as well as exhumation and erosion) have come to mean different things to different people, depending on their point of view, or particular application. England and Molnar (1990) and Summerfield (1991) wrote down some basic definitions for uplift and denudation, respectively, and here we follow their general terminology.

Uplift is defined as a displacement relative to the gravity vector and is the consequence of force(s) doing work against gravity. Furthermore, uplift needs to be expressed relative to a reference level. This is typically defined as mean sea level, or more correctly, the geoid (an equipotential surface, where gravity is the same everywhere). Uplift can be considered in terms of surface uplift, rock uplift and exhumation (although this term needs to be defined appropriately too), as illustrated in figure 1.

Surface uplift (U_s): displacement of the Earth's surface with respect to the geoid

Rock uplift (U_r) : displacement of a rock with respect to the geoid

Exhumation (U_e) : displacement of a rock with respect to the Earth's surface.

There is a simple algebraic relationship between these 3 , given as

$$U_s = U_r - U_e \quad (1)$$

Confusion has arisen in the geological literature where these terms are misused (e.g. by implicitly assuming $U_r = U_s$, which is only true if $U_e = 0$, and also by neglecting the role of isostasy (we return to this aspect later). In terms of understanding uplift resulting from tectonic forces, we are primarily interested in surface uplift. Often, however, absolute values and rates of uplift are quoted when the authors really mean exhumation or rock uplift.

Numerically, surface and rock uplift are equivalent if there is no erosion, and generally this requires us to consider a rock at the surface. In practice, beach deposits currently at 1000m elevation are a good indication of 1000m of *integrated* vertical motion since deposition (integrated because the surface and rock may have gone up to 2000m then back down to 1000 m).

One trivial consequence of uplift is that the uplifted region is higher than the surrounding area. One less trivial consequence is that the uplifted region has excess potential energy, and this emphasises the role of doing work against gravity. In terms of understanding the role of tectonic forces in generating topography, we need to consider surface uplift in the strict sense defined above.

Let us consider now a plateau region with thickened crust and its adjacent lowlands (figure 2). These two regions may both be in isostatic equilibrium, or having equal pressure at the compensation depth, z_c. (which requires the mountain to have a low density root). However, the pressure in each region will vary as a function of depth,

creating a difference in horizontal force, down to the compensation depth. The force (per unit of horizontal area) is related to pressure (P) through an integral over depth (z) so,

$$F = \int_0^{z_c} P(z)dz \tag{2a}$$

or

$$F = \int_0^{z_c} \rho g dz \tag{2b}$$

where ρ is density and g is the gravitational acceleration.

The horizontal force associated with the thickened crust (of thickness H_c) is

$$F1 = \frac{1}{2}\rho_C g H_C{}^2 \tag{3a}$$

and for the normal thickness crust (of thickness $H_c{}^0$) is

$$F2 = \rho_C g H_C^0 \left(H_C - h - \frac{1}{2}H_C^0 \right) + \rho_M g \left(H_C - h - \frac{1}{2}H_C^0 \right)^2 \tag{3b}$$

where ρ_M and ρ_C are the density of the mantle and crust respectively, and we have

$$\left(H_c = H_c^0 + \frac{h\rho_M}{\rho_M - \rho_C} \right) \tag{3c}$$

The net horizontal force is given as

$$\begin{aligned} FR &= F1 - F2 \\ &= \rho_C g h \left(H_C^0 + \frac{\rho_M h}{\rho_M - \rho_C} \right) \end{aligned} \tag{3d}$$

The difference in the force is such that the stresses are tensional in the elevated crust and compressional in the adjacent highlands. It is significant that the force difference increases as the square of the elevation.. Therefore, we can envisage there will be a limit to the elevation that can be constructed before the strength of the crust/lithosphere is exceeded. For reasonable values of the density terms ($\rho_C \sim 2700$ kgm^{-3}, and $\rho_M \sim 3300$ kgm^{-3}), we can generate kilobar stresses with about 3km of topography and 2 kilobars with 5 km. In general, we do not expect the Earth's crust to be able to support much larger stresses. Furthermore, these calculated forces give some indication of the amount of work (against gravity) required to create topography. Again, the dependence on the square of the elevation is critical as it means that it gets harder and harder to increase the elevation by a given amount as the elevation increases. Faulting can occur because it is easier (requires less work or energy) to fail than create higher topography. In this situation, the elevated region can grow in width rather than height (the required work increases linearly with width) and various styles faulting can occur, depending on the locality in the growing plateau. Typically, we expect thrusting at the margins and extensional faulting in the centre (e.g. in the Tibetan Plateau). Note the above statements require a large number of simplifying assumptions, such as the operation of local isostasy and that stress and strain are linearly related).

Denudation is a surface process that leads to the removal of material from the Earth's surface, and generally leads to a lowering of the surface (with respect to sea-level). Material may be removed in solid form or solution, and these two situations can be referred to as mechanical denudation (or *erosion*), and chemical denudation (or *weathering*) respectively. *Exhumation*, as defined in physical geography, refers to

exposure of a relict surface or palaeosurface, i.e. one that was buried under a cover, and this cover was subsequently removed. However, in the geological literature, exhumation is typically used to refer to the process by which rocks are brought from depth to the Earth's surface (e.g. England and Molnar 1990, Willett and Brandon 2002). While this may be regarded as purely a semantic difference of little consequence in the definition of uplift, it is important to be aware that such differences exist when dealing with different forms of data to constrain erosion/exhumation/denudation, an aspect discussed later.

As described above, uplift can lead to extension (e.g. Platt and England 1994) - and extension (with movement on normal faults) can lead to footwall rocks being brought from depth to the surface. This is often referred to as *tectonic denudation*, and is relevant to the situation where rocks on the footwall of a normal fault are exposed as a consequence of tectonic processes. In contrast, the phrase *erosional denudation* has been used to refer to the response to surface processes. The general geomorphological terminology would categorise these two as endogenic (internal) and exogenic (external) processes respectively (Summerfield 1991). In general, it seems erosional denudation is typically slower than tectonic denudation, although both can occur together (e.g. Wheeler and Butler 1994), and they can be difficult to separate. Erosional denudation can lead to further long wavelength uplift because of isostatic rebound, the magnitude of which depends on the effective strength of the lithosphere (e.g. Molnar and England 1990, Gilchrist and Summerfield 1991). We return to this later.

CAUSES OF UPLIFT

Analogous to the mechanisms that produce accommodation space in sedimentary basins, the causes of uplift can be broken down broadly into thermal, loading and stress-based factors, although all can operate to varying degrees. Typically these factors lead to density variations in the Earth's crust and upper mantle, and the isostatic response to these density variations leads to vertical motion of the Earth's surface. In terms of the processes involved in producing uplift it is useful to discriminate between transient and permanent uplift. In this sense, transient uplift disappears once a driving force is removed, and the rate of decay depends on the nature of the mechanism. Permanent uplift remains indefinitely, in the absence of any other forcing or modifying factors. In the following section we consider some simple formulations to quantify the surface uplift, generally assuming local isostasy operates unless stated otherwise.

Stress mechanisms

Compression is commonly invoked as a mechanism to produce uplift and this can be a consequence of both crustal and whole lithosphere thickening. Under appropriate conditions extension can also produce uplift. Similarly, compression can lead to subsidence. The sense of motion in response to applied stress depends on the initial and final density structure of the lithosphere. In general the crust has lower density than the underlying subcrustal lithospheric mantle, which itself is generally more dense than the sub-lithospheric mantle, or asthenosphere. Therefore, crustal thickening alone tends to reduce the average density of the lithosphere, and leads to uplift, while thickening of the sub-crustal lithosphere alone will tend to produce subsidence. Thinning of the whole

lithosphere can lead to uplift, if the initial crust is thin enough. Thickening of the whole lithosphere may produce subsidence or uplift depending on the relative contribution to the average density from the crust and sub-crustal mantle, which itself depends on their thicknesses and densities.

A basic relationship that allows us to quantify this is discussed by Stuwe (2002) for the elevation change, H

$$H = \delta h_C (f_C - 1) - \xi h_L (f_L - 1) \qquad (4a)$$

where h_c, and h_l are the reference crustal and lithosphere thickness (prior to thickening or thinning), f_c and f_L are the ratios of the initial to final thickness of the crust and lithosphere, respectively, δ is determined from the density of the crust (ρ_C) and mantle (ρ_M), i.e.

$$\delta = \frac{\rho_M - \rho_C}{\rho_M} \qquad (4b)$$

and ξ allows for the change in density due to the thermal structure defined by the temperature at the top and base of the lithosphere, T_S and T_L, i.e.

$$\xi = \frac{\alpha}{2}(T_L + T_S) \qquad (4c)$$

where α is the volume thermal expansion coefficient. The vertical motion predicted from this formulation is given in figure 3. This illustrates how homogenous thickening produces relatively little uplift, and the thickening of the low density crust trades off with thickening of the high density mantle. Thinning of the whole lithosphere generally leads to subsidence (if the initial crustal thickness is greater than about 15 km, McKenzie

1978), as does thickening of just the mantle. Thickening just the crust leads to uplift, and the highest magnitude uplift is produced by thinning the mantle while simultaneously thickening the crust. This latter situation may arise during compression, followed by delamination (e.g. Houseman et al. 1981, Platt and England 1994).

In-plane forces (both compression and tension) can lead to uplift (and subsidence). If the lithosphere, or part of it, behaves as an elastic or viscoelastic plate and has a pre-exisiting deflection, then an applied inplane force acts through the plate curvature as a vertical applied load (Lambeck 1983). Thus, a flexural bulge or trough will increase in amplitude under compression, while both tend to flatten out under tension. This mechanism has been invoked as an explanation for rapid apparent sea-level change (Cloetingh et al. 1985). In general, the amount of surface uplift for an elastic plate model in response to kilobar levels of in-plane compression is relatively small, tens to a few hundred metres. If viscous relaxation is important, then it is possible to produce larger amounts of uplift, at a rate determined by the viscous time constant of the lithosphere (e.g. Lambeck 1983).

Thermal mechanisms

Thermal driven uplift occurs when lithospheric material becomes hotter or when hot material replaces colder material. For the first case, assuming a constant density for the lithosphere ($\rho_{\square}$) and that the average temperature change over a thickness h_L is ΔT, the amount of uplift, H, is given as

$$H = h_L \frac{\Delta \rho'}{\rho_{st}} \qquad (5a)$$

where $\Delta\rho$' is the density difference for the material before and after the temperature change, and ρ□' is the density after the temperature change, given as

$$\rho_L^{'} = \rho_L(1 - \alpha\Delta T) \qquad (5b)$$

This leads to transient uplift, which disappears as the hot material cools. The rate of cooling is determined by the diffusivity (κ), and the length scale of the system (L), with a time constant, τ, given as

$$\tau = \frac{L^2}{\pi^2\kappa} \qquad (5c)$$

For lithosphere of thickness 120 km or so, this is equivalent to about 60 m.y. (with $\kappa \sim 32$ km m.y.$^{-2}$)

When material of a given density, ρ_1 is replaced by material of a different density, ρ_2, over a thickness interval h_L, the elevation change is given as

$$H = h_1\frac{(\rho_1 - \rho_2)}{\rho_M} \qquad (6)$$

This relationship is appropriate to magmatic underplating (McKenzie 1984), where low density melt or melt residue replaces the upper mantle at the base of the lower crust. This mechanism can produce permanent, long wavelength uplift.

Thermally driven dynamic uplift can occur in response to mantle convection. Considering a thermally driven mantle plume, for example, and following Davies (1998), it is straightforward to show that the relationship between uplift (per unit area) and heat loss (Q) is

$$H = \frac{\alpha Q}{\rho_M C_P}$$

where C_p is the specific heat capacity at constant pressure for the mantle rocks. Removal of dynamic support will obviously lead to subsidence, at a rate effectively equal to removal of the support (e.g. Houseman and England, 1986). In the absence of an obvious tectonic mechanism, Rohrman et al. (2002) have argued that the apparently recent (Cenozoic) uplift of parts of the North Atlantic margins, in particular southern Norway, is the result of thermal buoyancy due to mantle upwelling. Supporting evidence for this mechanism was the presence of seismically slow region between 50 and 250 km depth. Mitrovica et al. (1989) have shown how induced convection in the mantle wedge above a subducting plate can lead to subsidence of the continental interior and, similarly, once this dynamic mechanism ceases, the system responds in the opposite sense, i.e. uplift will occur. This appears to have been the case in Eastern Australia during the late Cretaceous, where prolonged subsidence of the continental interior abruptly ceased, and was succeeded by denudation (Gallagher et al. 1994),

Transient thermal uplift can also occur at rift margins, as a consequence of the rifting process itself. The introduction of relatively hot mantle in the rift zone against colder mantle/crust in the rift margins leads to lateral heat transfer from the former to the latter (Cochran 1983). This reduces the mean density of the unrifted region, and through isostasy, there will be surface uplift. Similarly, the initially hot mantle at the edge of the rift zone will cool, and tend to sink setting up secondary convection cells, which can produce dynamic uplift of the rift flanks (Buck 1986). Both methods lead to uplift on the order of a few hundred metres. As the whole rift system cools and thermal subsidence ensues, so to the thermally driven uplift decays with a similar time constant as the subsidence (typically 60-70 Ma). Consequently, these mechanisms cannot explain the

presence of apparently long lived (or permanent) uplift at old (> 100 Ma) rift margins such as the South Atlantic, but may be relevant to younger margins like the Red Sea.

Loading/unloading mechanisms

In general, loading of the lithosphere causes subsidence. However, if regional isostasy (in the sense of flexural support of applied loads) operates then uplift can occur in the form of peripheral bulges in response to surface loading. This effect is a well known consequence of the ocean island loading situation (e.g. Lambeck and Nakiboglu 1981) and also occurs in front of thrust belts, on the outer margin of the evolving foreland basin (e.g. Beaumont 1981). The magnitude of surface uplift at the flexural bulge is relatively small (10-100m), but may be enough to modify the proximal stratigraphy of the evolving foreland sedimentary basin.

Tectonic settings where flexural uplift in response to a combination of in-plane stress and loading is potentially important are rift settings. In this case, the mass redistribution due to extension produces buoyancy forces which can lead to uplift of both the basin and the rift flanks. As shown by Braun and Beaumont (1989), the important parameter is the necking depth (figure 4a) which is effectively a reference level about which thinning occurs. If the necking depth is deeper than the isostatic compensation depth, then uplift can occur (figure 4b), while if it is shallower then subsidence occurs (figure 4c). The mass redistribution due to what is referred to as the intrinsic necking needs to be considered before determining the isostatic response to changes in lithospheric density. Superimposed on the regional isostatic response is the geometrical change in crust/lithospheric thickness laterally. In the canonical pure shear model

(McKenzie 1978), this reference level is at the surface, and in this case extension introduces a mass excess relative to the necking depth. The flexural response leads to a broad zone of subsidence and an overdeepened basin. However, if the necking depth is deeper than the depth of compensation, then the isostatic response can lead to a broad uplift enough such that the rift flanks are elevated and the basin is shallower than expected.

Another secondary mechanism for local uplift, but relevant to the unloading mechanism is uplift related to denudation unloading. Denudation leads to mass removal so isostatic rebound occurs in response. Consequently, to denude an Airy isostatically compensated plateau at elevation H to sea-level requires denudation in excess of H. This is because the crust needs to be thicker under the plateau than the surrounding regions, i.e. there will be a crustal root whose excess thickness needs to be removed also. Assuming local isostasy, the appropriate expression for the rebound R and the total denudation D are

$$R = H\frac{\rho_C}{(\rho_M - \rho_C)} \tag{8a}$$

and

$$D = H\frac{\rho_M}{(\rho_M - \rho_C)} \tag{8b}$$

For the typical crustal and mantle densities mentioned before, this implies equivalent denudation of 5-6 times the elevation. The isostatic response is wavelength dependent, and for length scales in excess of 100-200 km, local (Airy) isostasy is generally appropriate. Therefore, for regional, but spatially variable denudation, it is possible to increase local peak heights (which do not erode), by removing material from intervening

valleys (e.g. Molnar and England 1990, and figure 5a) although this process cannot continue indefinitely, as the valley sides will tend to become gravitationally unstable.

Erosional unloading can also lead to uplift outside the region of unloading if the earth responds to unloading by flexure, as demonstrated by Gilchrist and Summerfield (1991) in the context of passive margin scarp retreat (figure 5b). For the case of flexure, the relationships analogous to those above are best expressed in the wavenumber domain (k is wavenumber, proportional to the inverse of wavelength), and we have the responses as a function of wavenumber as :

$$R(k) = H(k)\left[\frac{g\rho_C}{Nk^4 + g(\rho_M - \rho_C)}\right] \tag{9a}$$

and

$$D(k) = H(k)\left[\frac{Nk^4 + g\rho_M}{Nk^4 + g(\rho_M - \rho_C)}\right] \tag{9b}$$

where N is the effective flexural rigidity of the mechanical lithosphere. When N = 0, these reduce to the expressions above for Airy isostasy, and as N becomes large, then there is no rebound, and the required amount of denudation is equal to the elevation. These relationships demonstrate that the response is a function of wavelength (for constant N), and short wavelength (large k) features tend to be uncompensated, while long wavelength (small k) features tend to be compensated by local, or Airy, isostasy.

QUANTIFYING DENUDATION

Uplift will typically lead to changes in relative base-level for rivers and also in drainage systems, perhaps allowing previously unconnected systems to merge (drainage capture), or dividing/diverting an existing drainage system. This can then lead to changes in denudation rate and sediment/solute delivery to connected depositional basins. Furthermore uplift can lead to changes in atmospheric circulation (e.g. Ruddiman and Kutzbach 1989), which in themselves can modify denudation. However, as noted earlier, uplift does not necessarily lead to denudation, and even when it does, the temporal relationship may not be straightforward. Here we do not consider potentially direct indicators of uplift such as palaeobotany (e.g. Wolfe et al. 1997), stable isotopes in authigenic minerals (Page Chamberlain and Poage 2000) or vesicle size in lavas (Sahagian and Maus, 1994). These interesting methods have not been widely applied, and their applicability over geological timescales is complicated, partly due to removal by denudation, or uncertainty regarding other factors such as climatic effects (for palaeobotany). Although climate change and surface uplift undoubtedly have the potential for exhibiting complex feedback behaviour, which is beyond the scope of this chapter.

In sedimentary basins, the geological timescale record of vertical motion is at least partially preserved through the stratigraphy. In contrast, uplifted regions tend to be eroded and remove any direct record of vertical motion. Consequently, one of the key issues is how to constrain uplift. As mentioned earlier, there is a degree of confusion concerning uplift and erosion. In general, it is erosion that is inferred, and then (mistakenly) referred to as uplift, although this is just the exhumation term defined in 1.

Qualitative denudation chronologies in the more traditional geomorphological sense, based on correlating surfaces, are still used in recent work. For example, Partridge and Maud (1987) have applied this concept in South Africa, Lidmar-Bergstrom and Nalsund (2002) in Scandinavia, and Widdowson (1997) in India. Often, there many problems inherent in this approach and great care is required with field observations. Summerfield (2000) presents the historical context for the development of these chronologies and discusses some of the main problems. These include the uncertainty inherent in correlating palaeosurfaces over large distances, effectively ignoring tectonics and isostasy, the difficulty in resolving structural and lithological controls from baselevel changes, and the difficulty in dating weathering surfaces and timing overall. Although Vasconcelos (1999), and Shuster et al. (2005) discuss the application of radiometric dating to this problem, they have yet to be widely applied. We do not consider denudation chronologies based essentially on visual inspection in this chapter.

Here, we consider some of the more common *quantitative* approaches for the inference of denudation operating over geological timescales (e.g. timescales in excess of 100,000 years) and depth scales of up to a few kilometres (1-2 kbars). These approaches include techniques which are sensitive to the exposure time of a surface (to cosmic rays), techniques which are sensitive to temperature (as denudation generally leads to cooling of a rock as it approaches the Earth's surface), those sensitive to pressure (which reduces as overburden is removed), and, less commonly applied, those which infer erosion from the discrepancies between observed and theoretical subsidence in sedimentary basins. In table 2 we briefly summarise an example of each method we discuss in the subsequent sections, and the references provide other examples of applications.

Exposure Age Methods

The exposure time methods are known under the umbrella term of cosmogenic surface exposure dating, and rely on the interaction of secondary cosmic rays (predominantly neutrons produced by the interaction of primary cosmic rays and the Earth's atmosphere) with atoms in common minerals (e.g. quartz, olivine,feldspar) in the upper metre or so of the Earth's surface. When secondary cosmic rays (fast neutrons) interact with rocks, spallation reactions occur, producing elements (daughter isotopes) of lower atomic number than the parent element. Lower energy particles (thermal neutrons) can also produce new isotopes by neutron capture, which can lead to both heavier and lighter daughters. The new cosmogenically produced isotopes may be radioactive (^{26}Al, ^{10}Be, ^{36}Cl) or stable (^{21}Ne, ^{3}He).

The daughter element formed depends on the parent element, in turn dependent on the mineral host. Typical pairs are shown in table 1, together with the half-life where appropriate. The depth to which cosmic rays penetrate solid rock depends on the type of particle, but the more common particles will only reach 1-2 m, before becoming effectively undetectable. Muons can travel further, perhaps as much as 50 m or so. The attenuation of rays depends on the density of the material but follows an exponential function of depth. As the rays are attenuated with depth, so to then is the production of the daughter isotopes (figure 6a) and the production rate follows essentially the same form as that given above

$$J(z) = J_0 e^{-z/z^*} \tag{10}$$

where z is depth, J_0 is the surface value production rate and z* is a characteristic depth scale for the material of interest (which depends on the density).

In addition, as the cosmic ray flux depends on latitude and elevation, then so too does the daughter production rate. For a constant altitude, cosmic rays are more attenuated at the equator than the poles. Furthermore, the Earth's magnetic field varies not only spatially but also with time. As the field changes, the variations in cosmic ray attenuation is more marked at the equator (i.e. the flux is more sensitive here), and similarly, the relative variations are greater at higher altitudes.

Gosse and Phillips (2001) recount an intuitive analogy (originally from Everson) to cosmogenic surface exposure dating through a comparison to obtaining a suntan. The intensity (degree of tan, measured abundance of cosmogenic nuclide) depends on elevation, latitude and exposure time, shielding (sunscreen, or ice, vegetation, rock cover) to prevent accumulation, The intensity depends on the nature of the material (skin type, mineral), repeated exposure can be cumulative and the loss of the surface material (skin peeling, erosion) affects the inference of exposure time, and the effect fades with time (for radioactive systems).

The relevant equation for the concentration of a cosmogenic radionuclide as a function of depth and time, assuming an initial concentration of zero and no additional sources, is

$$C(t) = \frac{J_0 e^{-z/z^*}}{E/z^* + \lambda}\left(1 - e^{-(E/z^* + \lambda)t}\right) \tag{11a}$$

where E is erosion rate and λ is the decay constant for a radiogenic isotope. For surface samples (z = 0), we have

$$C(t) = \frac{J_0}{E/z^* + \lambda}\left(1 - e^{-(E/z^* + \lambda)t}\right) \qquad (11b)$$

In the general case, there are two unknowns, the erosion rate, and the exposure time. For a single surface sample, we can fix one, and infer the other. In the case of zero or constant (and known) erosion, the age measures the duration of exposure. If zero erosion is assumed but is invalid, then the exposure age is a minimum value, and this age is a function of the erosion rate (figure 6b). The maximum value attainable for the exposure duration is a function of the decay constant for the radiogenic isotopes, which reach a steady state, or equilibrium value, reflecting the balance between production and decay as shown in figure 6. This is typically around 4-5 half-lives, and then the maximum time is around 5-6 m.y. (for ^{10}Be). Stable isotopes can accumulate progressively, but their interpretation over long timescales is complicated by the potential for burial and shielding.

The use of two isotopes in principle allows the inference of both erosion and exposure duration. The ratio of two isotopes is given as

$$\frac{C^1(t)}{C^2(t)} = \frac{J_0^1\left(E/z^* + \lambda^2\right)}{J_0^2\left(E/z^* + \lambda^1\right)}\frac{\left(1 - e^{-(E/z^* + \lambda^1)t}\right)}{\left(1 - e^{-(E/z^* + \lambda^2)t}\right)} \qquad (12)$$

The only differences between the terms are in the decay constants and the production rates. Thus, to be useful, these need to differ between the two isotopes. An isotope with a longer half-life takes longer to reach the steady state value, for a given erosion rate. The

shorter half life isotope can be used to infer the erosion rate, and the longer (non-steady state) isotope, or a stable isotope can be used to infer the exposure age (see Gosse and Phillips 2001). Cockburn et al. (2000) combined ^{10}Be and ^{26}Al to determine denudation and scarp retreat rates for the Namibian passive margin. Given the distance from the escarpment to the passive margin edge, a constant rate of retreat implies ~1 km/m.y. The measured denudation and retreat rates were far too low (< 20m/m.y. and < 10 m/m.y.) to be consistent with a constant rate of scarp retreat since continental break-up 130 Ma. They concluded a downwearing model with a pinned internal drainage divide was more appropriate.

The potential for using cosmogenic isotopes to infer uplift directly has been considered, as the production rate is a function of elevation. Consequently, the ratio of the present day production rate to that at time t, is given as

$$\frac{J_0(0)}{J_0(t)} = e^{-u^*/z^*}$$

where u* is the uplift rate – erosion rate, and here z* is the atmospheric attenuation rate of cosmic rays. In practice, the production rate is difficult to constrain (Dunai 2000), and to date, this approach has had only limited success.

In contrast, the application of cosmogenic methods to sediments has grown significantly over the last few years (e.g. Granger et al. 1996, Clapp et al. 2002). The motivation for this is that the sediments sample a broad region of the eroding catchment, and so provide an integrated representation of the regional denudation rate, compared with single location samples in bedrock, which can lead to very site specific estimates. Obviously, the two approaches have their merits in different situations.

Comprehensive reviews of cosmogenic surface exposure dating are provided by Cerling and Craig (1994), Gosse and Phillips (2001), Bierman and Nichols (2004), and Summerfield and Cockburn (2004), and these papers cite many applications and examples.

Temperature sensitive methods

The relevant temperature-sensitive methods include apatite fission track analysis, (U-Th)/He dating of apatite, and vitrinite reflectance. There are other methods , such as the illite-smectite transformation, but these are not as widely applied in this context. The former two of these provide information on the thermal history of a rock (this is referred to as thermochronology), while the latter two provide only information the maximum temperature of the rock. Furthermore, the former two can be applied to both in basement and sedimentary basin settings, while the latter two are pretty much limited to sediments. All methods can be applied to surface samples, as well as samples from drill holes down to the level where the system is no longer sensitive. In practices this is 2-6 km depth depending on the method and the temperature gradient.

Apatite fission track thermochronology

The basics of apatite fission track (AFT) thermochronology have been summarised in Gallagher et al (1998) and here we provide a brief overview drawn from this earlier publication. Fission tracks are linear damage features formed from the spontaneous

fission of ^{238}U, which occurs in trace amounts (10-100 ppm) in apatite. A typical fission reaction can be written in terms of the mass of the fragments as

$$^{238}U \rightarrow {}^{90}Kr + {}^{143}Ba + Q \qquad (14)$$

where Q is energy. The decay products are large ions (not alpha particles), and these repel each other, stripping electrons from nearby atoms in their paths, leaving a linear damage trail in the crystal lattice that is a *fission track*. This spontaneous fission of ^{238}U occurs at a constant rate over time, so this system can be used for dating, in the same way that any radioactive decay system. In this case, the parent is ^{238}U and the daughter produced is a fission track. An age can be determined by counting the number of tracks and measuring the present day uranium content.

When first formed the tracks are more or less constant length (~17 μm), although they seem to rapidly shorten to around 16 μm within a few weeks at room temperature (Donelick et al. 1990). Tracks are metastable and are particularly sensitive to temperature, and less to time. The consequence of this sensitivity is that that a given track becomes progressively shorter, with relatively minor amount of radial shrinking – this is known as annealing. This process means that the daughter product (i.e. tracks) can disappear, and so the estimated age will be younger than the true age of the host mineral. Therefore, to understand the significance of the fission track age, it is critical to know the underlying track length distribution. Thus, a typical fission track analysis produces two types of basic data – single grain ages, and track length distribution (typically sampled from individual tracks in many crystals). The former provides information on timing, and the latter provides information on the temperature, so together these data allows us to

reconstruct the thermal history of the host rock. As denudation leads to cooling, in many cases the thermal history can then be used as proxy for denudation history.

Laboratory experiments and geological case studies have been used to constrain the temperature and time dependence, Based on these experiments, empricial annealing models have been developed, and a typical mathematical representation for isothermal annealing is (Laslett et al. 1987)

$$g(r) = c_0 + c_1 T(\ln(t) + c_2) \qquad (15a)$$

with

$$g(r) = \frac{\left(\left(1 - r^b\right)/b\right)^a - 1}{a} \qquad (15b)$$

where r is the reduced track length (the length normalised by the initial, unannealed length), and T is temperature (K), and t is time (seconds), and the other terms are empirically derived constants. Other formulations have been presented by Carlson (1990), Laslett and Galbraith (1996) and Ketcham et al. (1999). These also involve a similar log time : linear temperature dependence to that given above. The models calibrated by Ketcham et al. (1999) differ from other published models in that they explicitly allow for compositional variation (in particular the influence of variable chlorine and fluorine contents - tracks in fluorine rich apatite anneal more rapidly than those in chlorine rich apatite). The temperature range over which annealing occurs is known as the partial annealing zone (PAZ). For geological timescales (1 - 100 m.y.), the upper limit of the PAZ is around 110-120°C, and tracks are effectively annealed instantaneously above this. The lower limit is generally taken to be 50-60°C, although

this is less well defined, and it is clear that there is some annealing below this temperature range (e.g. Vrojlick et al. 1992).

The empirical annealing models allow prediction of the expected length of a given fission track at the present day for a specified thermal history. As fission tracks form continually over time, then each one will experience a different proportion of the total thermal history of the host mineral. We can simulate the response of each track to a given thermal history, and predict the length distribution and fission track age (e.g. Green et al. 1989, Ketcham et al. 1999). Fission track data are most informative when dealing with cooling, as each successively young track experiences a different temperature maximum, and so a complete analysis provides detail on the nature of the cooling history (figure 7b). In contrast, a continuous heating thermal history, where the present day temperature is a maximum, really only tells us that we are at the maximum temperature today (figure 7a).

Given that we can forward model the fission track data by specifying a thermal history, it is then possible to infer the thermal history directly from observed fission track data (Gallagher 1995, Willett 1997, Ketcham et al. 2000). In order to convert the inferred thermal history to an equivalent depth, it is commonly assumed that transient thermal effects and 2D/3D heat transfer are not significant. Then it is necessary simply to assume a surface temperature (T_s) and adopt either a temperature-depth gradient (dT/dz), or heat flow (Q) and thermal conductivity (k). The relationship between these two is given by Fourier's law,

$$Q = k\frac{dT}{dz} \qquad (16a)$$

and the depth, Z_T equivalent to a give temperature T_Z is given as

$$Z_T = \frac{(T_Z - T_s)}{dT/dz} \tag{16b}$$

or

$$Z_T = (T_Z - T_s)\frac{k}{Q} \tag{16c}$$

Typically, temperature gradients of 25-20°C/km are adopted often with little justification other than these are more or less normal values. However, as the thermal conductivity of rocks can vary by a factor of 2-3, then if there are independent data on thermal conductivities, and the heat flow, this is generally a preferable approach.

Gallagher et al. (1998), Dumitru (2000), Gleadow and Brown (2000), provide reviews of fission track analysis, and their application to denudation modelling, while Gunnell (2000) reviews the methodology from a geomorphological viewpoint. More specifically, Brown et al. (2000), Gunnell et al. (2003) and Kohn et al. (2002) present results of modelling regional denudation based on apatite fission track analysis from surface samples in Africa, South America, India and Australia. Brown (1991) outlines how to 'backstack' the estimated denuded section back on the present day topography to try and infer the change in elevation. Fitzgerald et al. (1995) used vertical profile samples over an elevation range of 4.5 km to infer rapid cooling (and denudation) in a relatively restricted region (effectively a single mountain) in an attempt to infer absolute uplift using backstacking. They inferred 8.5 km of rock uplift, 5.7 km of denudation and 2.8 m

of mean surface uplift, at rates of ~1.5, ~1 and 0,.5 km/m.y., respectively. Green et al. (1995, 2002) consider the application of apatite fission track analysis from borehole and surface samples to constrain inversion of sedimentary basins, often a key unknown in hydrocarbon exploration.

Apatite (U-Th)/He dating

This method relies on the production of helium (as alpha particles) from uranium and thorium. The relevant decay systems are

$$\begin{aligned} {}^{238}U &\rightarrow {}^{206}Pb + 8\,{}^{4}_{2}He \\ {}^{235}U &\rightarrow {}^{207}Pb + 7\,{}^{4}_{2}He \\ {}^{232}Th &\rightarrow {}^{208}Pb + 6\,{}^{4}_{2}He \end{aligned} \qquad (17)$$

This was proposed as a dating method by Rutherford in 1908, but it was quickly realised that the ages were anomalously young as a consequence of thermally activated diffusive loss of helium. Zeitler et al. (1987) suggested exploiting the temperature sensitivity to use apatite (U-Th)/He for thermochonology, in a manner similar to fission track annealing. Diffusive loss of helium occurs over a temperature range, known as the partial retention zone. For geological timescales, the partial retention zone of helium ion apatite is around 40-80°C, based on the extrapolation of laboratory diffusion experiments (Wolf et al. 1996, Farley 2000). Thus, the partial retention zone overlaps with the partial annealing zone of fission tracks in apatite (figure 8). This has been demonstrated in geological settings by House et al. (1999), using borehole samples from volcanogenic sediments in

the Otway Basin, Australia, and by Stockli et al (2000) on basement rocks from an exhumed fault block in California.

The helium concentration, C, (as a function of time, t, and position, r) is given as

$$\frac{\partial C(t,r)}{\partial t} = D(t)\left(\frac{\partial^2 C(t,r)}{\partial r^2} + \frac{n}{r}\frac{\partial C(t,r)}{\partial r}\right) + P(t) \qquad (18a)$$

where P(t) the production rate of helium (from the decay equations above), and n is constant whose value is determined by the geometry of the system being modelled (n = 2 is a sphere, n = 1 is an infinite cylinder, and n = 0 is an infinite sheet). D(t) is the temperature dependent diffusion coefficient, given as

$$D(t) = D_0 e^{-\frac{E}{RT}} \qquad (18b)$$

where E is activation energy, R is the universal gas constant and T is absolute temperature. For a single analysis (which may or not involve individual crystals), the (U-Th)/He system does not provide as much direct information as a single apatite fission track analysis. Similarly, the interpretation of a single helium age is difficult, unless the sample cooled rapidly through the partial retention zone. However, multiple analyses (involving either single grains, or grains of similar size) have great potential, if a range of different grain sizes can be analysed (Reiners and Farley, 2001). This is because the diffusion domain for helium in apatite appears to be the whole crystal. Consequently, the measured age and effective closure temperature is a function of the grain size, with smaller grains expected to have younger ages (and lower closure temperatures) than larger grains.

Farley (2000), Reiners (2002) and Ehlers and Farley (2003) provide reviews of the methodology and application of (U-Th)/He dating as a thermochronological tool, and it should be noted here that future research will also focus on zircon and sphere (U-Th)/He analysis, although these systems are currently not as well characterised as apatite. This method was has not yet been widely applied in sedimentary basin settings, but as a consequence of the very low temperature sensitivity, has provided useful constraints for topographic evolution in terms of relief changes. For example, House et al. (1998) used the method to infer the timing of relief change (valley cutting) in the Sierra Nevada, California. This exploited the facts that isotherms close to the surface are warped due the topography, and leads to horizontal variations in temperature between ridges and valleys. The results implied deep valleys and the high topography had developed by the late Cretaceous, some 50-60 Ma older than previously thought. Braun (2002) developed a method for exploiting regional data sets to infer the timing of relief change, based on the correlation of topography and (U-Th)/He ages over different wavelengths.

Vitrinite reflectance

Vitrinite is a common type of organic matter whose reflectance increases with increasing temperature and it is widely used in the hydrocarbon exploration industry as an indicator of the temperature of hydrocarbon source rocks. The reflectance is measured with a microscope under oil immersion and photomultiplier, and is expressed as a percentage in terms of reflection of the incident light, usually written as %Ro. A variety of different

models have been proposed to relate vitrinite reflectance to temperature, but a discussion of the validity of these is beyond the scope of this paper. Morrow and Issler (1993) have assessed a variety of commonly used vitrinite models. They recommend the kinetic model of Burnham and Sweeney (1989), which is based on a series of first order Arrhenius-type reactions, i.e.

$$\frac{dC}{dt} = -kC \tag{19a}$$

where C is the concentration of the reactant and k is the rate constant given as

$$k = Ae^{-\frac{E}{RT}} \tag{19b}$$

where A is the pre-exponential, or frequency, factor, and the other terms have been defined earlier. The reactions simulate the breakdown of vitrinite as follows

$$vitrinite \rightarrow residual vitrinite + product \tag{20}$$

where the products are CO_2, H_2O, CH_4 or a general hydrocarbon, CH_n. The reactions are assumed to be independent, and parallel, with a distribution of activation energies for each reaction. The model is calibrated against vitrinite reflectance using the following relationship

$$\%Ro = 12\exp\left(-3.3\left(H/C\right)\right) - O/C \tag{21}$$

A major difference between vitrinite reflectance and apatite fission track analysis is that the former is essentially just a maximum temperature indicator, while the latter provides information on the temperature variation over time (figure 9). However, in sedimentary basin settings, the two methods are most useful in combination (Arne and Zentilli 1994).

This is partly because of practical considerations (apatite tends to occur in immature clastic sediments, while vitrinite is obtained from mud rocks), but also because the two systems seem to have important parallel behaviour in terms of their sensitivity to time and temperature. Furthermore, apatite in sediments can retain a provenance, or inherited, signature, while vitrinite does not. As vitrinite provides an indication of the overall maximum temperature of the rock sample, then this provides independent an constraint which aids in interpreting the potentially complex thermal history recorded in the apatite fission track data. Kamp et al. (1996), Ventura et al. (2001), Arne et al. (2002) and Green et al. (2002) integrated vitrinite reflectance and apatite fission track analysis to constrain timing and magnitude of basin inversion. In these studies, the combination of the two methods provided more information than either taken separately. Green et al. (2002), using a series of vertical samples, claimed to have resolved changes in heat flow as well as the response to denudation. Although there is clearly a trade-off between the two parameters, this is reduced if a series of samples over depth are used.

Pressure-sensitive methods

Probably the most widely applied pressure sensitive method relies on the progressive reduction of porosity in sediments due to burial. It is assumed that the porosity reduction is irreversible and follows a simple trend as a function of maximum burial depth. Subsequently, when denudation occurs, the sediment resides at a shallower depth, but the average porosity is less than expected for that depth, as a consequence of the removal of overburden. Assuming the relationship between porosity and depth is

known, then it is possible to estimate the maximum burial depth from the observed porosity (figure 10).

Typically, porosity (ϕ) as a function of depth (z) is parameterised in the following form

$$\phi(z) = \phi_0 e^{-cz} \tag{22a}$$

where ϕ_0 is the surface porosity, and c is length scale constant. Clearly, this relationship ideally needs to be defined in a region where there has been no denudation (or diagenetic alteration of porosity). An estimate of the amount of removed section can be made using the observed (ϕ^o) and predicted (ϕ^p) porosity at a present day depth, z,, the amount of denudation, D, is given as

$$D = \frac{-1}{c} Ln\left(1 - \frac{\left(\phi^p - \phi^o\right)}{\phi_0} e^{cz}\right) \tag{22b}$$

Commonly, sonic velocity data are used to estimate porosity (e.g.Bulat and Stoker, 1987, Hillis 1995, Japsen 1998). In this case, the basic porosity function given above is combined with the Wyllie et al. (1956) average velocity equation,

$$\frac{1}{V} = \frac{1-\phi}{V_{ma}} + \frac{\phi}{V_f} \tag{23a}$$

where V_{ma} and V_f are the rock matrix and fluid sonic velocities, respectively, to give

$$\frac{1}{V} = \frac{1}{V_{ma}} + \frac{(V_{ma} - V_f)}{V_{ma} V_f} \phi_0 e^{-cz} \tag{23b}$$

which can be linearised in z if c^{-1} is much greater than z to give

$$\frac{1}{V} = \frac{1}{V_{ma}} - \frac{(V_{ma} - V_f)}{V_{ma} V_f} \phi_0 cz \tag{23c}$$

Then, the maximum depth is given as

$$z^{\max} = \frac{1}{\phi_0 c}\left(\frac{1}{V_{ma}} - \frac{1}{V}\right)\frac{V_{ma} V_f}{(V_{ma} - V_f)} \tag{23d}$$

and the amount of denudation (missing section) is then the difference between z_{max} and the present day depth.

Alternatively, the thickness of the missing section can be expressed in terms of interval travel time as (Hillis 1995)

$$D = \frac{1}{m}\left(\Delta t_z - \Delta t_0\right) - z \tag{24}$$

where Δt_z is the interval travel time over the formation interval and Δt_0 and m are the surface intercept and slope of the linear depth- interval travel time relation defined for that particular formation. In the relationships above, the sonic velocity or travel time are taken as the mean of the appropriate interval represented by the formation under consideration, and the present depth is the mid point of the formation.

The method requires a reliable estimate of the normal compaction trend, which can be based on the highest measured porosities or the lowest sonic velocities over a given depth interval. To identify this background trend requires data from stable areas

often well outside the region of inversion. Then, we need to be confident that there are no significant lateral variations in the controls on porosity or the facies of a particular formation. If sediments have been buried, and later lost overburden, followed by reburial to a shallower depth than originally reached then this method will potentially underestimate the amount of section lost, unless the second phase of burial is corrected for (e.g. Hillis 1995, Japsen 1998).

If the second phase of burial is deeper than the first phase, then the record of the denudation will be overprinted. Similarly, it is not straightforward to reconstruct the total lost section after multiple phases of denudation and reburial. As shown by Hillis (1995), the relationship between the present day (z_p) depth, maximum burial depth (z_m), and the inferred missing section (Δz) is

$$z_m = z_p + \Delta z \tag{25}$$

Hillis (1995), Menpes and Hillis (1995), Japsen (1998), Densley et al. (2000), Ware and Turner (2002) have all exploited seismic velocity-depth anomalies to infer the magnitude of missing section around the North Sea, Irish Sea and Australia. In general, the applications use shale or chalk velocities, as these tend to be less variable than sandstones, as a consequence of diagenetic effects, or lack thereof. However, in Japsen (1995), he identified negative anomalies in chalk interval velocities in the central and southern North Sea, indicative of overpressure, such that porosity reduction was less than the normal compaction trend, or equivalent to underburial of ~1 km. The positive

anomalies imply up to 1 km over burden has been removed from the basin margins in the Neogene.

Subsidence methods

The final method we consider briefly is applicable in situations where the subsidence of a sedimentary basin can be expected to follow a predictable trend over time. The difference between the predicted and final depth of a given stratigraphic horizon in the basin then provides a estimate of the missing section. In practice, this method requires reliable assumptions concerning the tectonic mechanism driving subsidence. Generally, such assumptions are only convincingly valid in the extensional setting, as typified by the pure shear model of McKenzie (1978), and its variants. This approach relies on specifying the theoretical subsidence curve, either as a forward model, or undertaking some form of inverse modelling, using the observed subsidence as a constraint, and inferring the missing part of the section from the model predictions (Figure 11). In practice, this involves the usual approach to backstripping to determine the tectonic subsidence, i.e. allowing for compaction, sea-level and palaeobathymetry changes over time, and assuming some form of isostatic correction for the sediment load. In foreland basins, it is not possible to predict the subsidence history a priori unless the loading history is known and so this approach is not suitable, In extensional basins, it requires knowledge, or inference, of the extension history, and the relevant parameters required to predict the thermal subsidence phase. Rowley and White (1998) have shown that this approach tends

to give lower estimates of denudation (or missing section) than vitrinite reflectance or apatite fission track thermochronology, but the 3 methods are broadly consistent.

DENUDATION AND SEDIMENT SUPPLY

The products of denudation eventually end up in a sedimentary basin, The stratigraphy of a basin will clearly reflect the rate of sediment supply, which itself depends on factors such as relief, slope, climate, lithology, vegetation and runoff in the drainage catchment, all potential influences on denudation. This aspect is beyond the scope of this chapter, but Hovius and Leeder (1998) edited a special issue containing various modelling and case studies. However, another method to assess regional denudation is to consider the sediment volumes preserved in a basin as a proxy for the amount of material removed by denudation. This seemingly intuitive approach has some problems. Firstly, we do not know the area of the region that was denuded, so comparison of sedimentation and denudation rates is difficult and the size of both the source and deposition regions are likely to have changed over time. Secondly, denuded material may be removed in solution and/or transported away from an adjacent depositional basin. Conversely, the source region of the basin may have changed over time, and then it is not appropriate to associate the volume of sediments with one source. Finally, there may be some unknown time delay between denudation and final deposition, either due to storage in a drainage basin (or catchment), and so we do not necessarily expext a 1:1 correspondence in timing of denudation and deposition.

Historically, one region where sediments have been widely studied in the context of denudation are the North Alpine Foreland Basin in the European Alps. The basin is

characterised by arrival of deepwater flysch in the Alpine basins, and a widespread transition to the shallow water/continental molasse. The changes in lithology and water depth have been interpreted in terms of initial erosion of the orogenic wedge, followed by rapid influx, reflecting rapid uplift in the hinterland. Sinclair (1997) determined the erosion rate increased by about 30% during the flysch-molasse transition. However, this was under the assumption that the drainage area at the time is the same as the present day.

There are various approaches to try and fingerprint the source region. One of the approaches relies on looking at mineralogical assemblages and compositions (particularly heavy minerals, e.g. Mange and Maurer 1992, Morton and Hallsworth 1994, Morton and Hallsworth 1999, Morton et al. 2004) and linking the composition variation in sediments to that of potential source regions, or the mineral content of present day river sediments draining the source regions. The mineral groups considered need to be selected carefully, to allow for the potential of transport and diagenetic processes to filter the original detrital mineral population. Lonergan and Mange-Rajetzky (1994) exploited the sequence of heavy mineral assemblages of increasing grade in sediments deposited over ~10 m.y. in the Betics. The assemblages contained an inverted grade (relative to the sediment stratigrahy) and the maximum grade was equivalent to 30 km depth. Thus, they inferred a time-averaged erosion rate of 3 km/m.y.

Another approach is to date detrital minerals and again try to link these back to ages of the same minerals in potential source regions. The more commonly adopted dating methods use single grains and include U-Pb zircon, zircon fission track analysis, and $^{40}Ar/^{39}Ar$ dating of micas In all approaches, it is implicit that the mineral system has been closed after erosion. Bernet et al. (2004) give an overview of the application of

zircon fission track analysis to provenance studies, using samples from both the source region and modern sediments carried in rivers from the same drainage system. Carter and Moss (1999) combined detrital zircon fission track analysis with zircon U-Pb dating, to exploit the different temperature sensitivity of these two dating systems. The effective closure temperature for the first system is about 200-320°C, while for the second it is generally inferred to be in excess of 700°C. Similarly, Rahl et al. (2003) combined zircon (U-Th)/He (closure temperature around 180°C) with zircon U-Pb, and Garver et al. (1999) combined apatite and zircon fission track detrital ages for the same reasons. The combination of two methods with different sensitivity can be used to identify the primary source terrain, and subsequent thermal events that may have affected it. The application of Sherlock et al. (2002) demonstrates that single grain $^{40}Ar/^{39}Ar$ ages can be misleading in that even a single crystal can be zoned in argon due to a complex thermal evolution, while Brewer et al. (2003) showed that analytical uncertainty combined with spatial variability in the denudation rates can lead to misleading inferences from river sediment samples.

MODELLING REGIONAL DENUDATION

In the last 10 years or so, a major research effort in the Earth Sciences has focussed on developing quantitative regional scale models for denudation as it operates over geological timescales. The models can be broadly subdivided in those which address surface processes, and those which aim to combine surface process models with tectonics. Overall, these approaches come under the Earth Systems Science umbrella, which can probably be regarded as 21st century scientific discipline in its own right. In

more traditional terms, this is the integration of geology, geography, physics, chemistry, biology and mathematics to understand the interactions of the solid earth, atmosphere, hydrosphere and biosphere, addressing in particular the complex feedback systems that often emerge from modelling studies without prior specification.

The improving quality of Digital Elevation Model (DEM) has increased their application to studies of denudation. They can be used as a general reference frame for calculating mass balances (Mayer 2000), essentially filling in the present day valleys to a chosen reference level. They are also useful for quantitative comparison to landscape evolution model predictions, and as the starting condition or input to these models. In terms of specific applications, Dadson et al. (2003) correlated their various estimates of denudation rate with stream power calculated from a Digital Elevation Model (DEM) and precipitation, but found little to suggest that stream power is a factor on erosion over decadal timescales. Montgomery and Brandon (2002) analysed the link between slope, relief and long term erosion rates for both tectonically inactive and active regions using the GTOPO30 global DEM. They demonstrate that inactive regions conform to the well known linear relation between mean local relief and erosion rate of Ahnert (1970). In contrast, the more active areas show a non-linear relationship, with erosion rate increasing (in response to climate and tectonics) more rapidly than mean slope, which is limited by soil/rock strength. They conclude that the low relief areas are controlled by hillslope processes, while landsliding in response to tectonic forcing occurs when river incision keeps pace with rock uplift in high relief areas.

Although the development of quantitative surface process models began 20-30 years ago (Carson and Kirkby 1972), the major applications in the more geological areas

of Earth Science took off perhaps only 10 years ago (see Merritts and Ellis 1994), and this marked the beginning of regional scale modelling incorporating surface processes and tectonics, and to some extent climate. Since, then there have been many studies exploring these interactions and considering what can be learnt and constrained from modelling. In addition, there is a wealth of geomorphological literature that generally focusses on smaller spatial and length scales but, although significant, these studies are not as relevant in the present context. The numerical surface process models have focussed on processes such as fluvial incision leading to bedrock erosion (the rate of which which can be transport or detachment controlled), and hillslope diffusion (e.g. Braun and Sambridge 1997, Willet et al. 2001, Whipple 2001, Simpson and Schunlegger 2003). Among the main issues that that have been addressed are the significance of tectonics and climate in terms of producing surface uplift (e.g. Molnar and England 1990), as well as the relative importance of steady state and non-steady state conditions in landscape evolution (e.g. Willet and Brandon 2002).

A demonstration of the current high profile of climate-tectonics-denudation interactions is given in the three papers published in Nature in 2003 (Burbank et al. 2003, Dadson et al,, 2003, Reiners et al. 2003), together with an overview by Molnar (2003), who also discusses another study by Wobus et al. 2003). In essence, all adopt the same overall approach in terms of quantifying the spatial variation in denudation rate using thermochronological data and then relating this to the present day precipitation (or similarly short term records, such as stream power or seismicity). One potential limitation of this approach is these inferences relate to different timescales and implicit in these approaches is then the assumption of steady state (in terms of denudation and climate

control). The four studies reach different conclusions about the importance of tectonics and climate on denudation, and this questions is still open. Intuitively, however, we might expect that these different factors will vary in the significance, both in time and spatially, and so the search for a single unifying or global model is unlikely to prove fruitful, unless it captures these scale dependent phenomena.

The second aspect, regarding steady state, is similarly unresolved, and is also complicated by the large range of time and length scales which can be considered as well as nature of the system being regarded in terms of steady state (topographic, thermal, denudation – see Willett and Brandon 2002). Overall, the scale variation is such that some form of steady state may be approximated at one scale (e.g. long wavelength or mean elevation), while clearly not at another (local landsliding in river valleys). A recent commentary by Allen (2005), discussing the relative roles of continuity and catastrophe in landscape evolution, suggests that it is better to think in terms of response times. That is, landscapes will respond to different perturbations at different rates. If the response time is small compared to the periodicity of a perturbation, they will appear in steady state. If the response time is long, they will appear transient.

Some of the other notable large scale work includes that by Beaumont et al, (2000) which considered the coupling of surface processes to the evolution of different tectonic situations, including passive margins and convergent orogens, and demonstrates the potential for complex feedbacks, particularly for active orogens. Willet (1999) specifically focussed on the link between tectonics and climate in convergent orogens, and showed that the relative importance of vertical uplift and horizontal convergence exhibits a major control on the geomorphic evolution. Finally, van de Beek and Braun

(1998), and van der Beek et al. (2002) considered surface process models in the context of passive margin, and particularly the controls on escarpment retreat. In this case, the competing models are continuous horizontal scarp retreat, and vertical downwearing. The important factor the location of the drainage divide which, if located inland of the escarpment, can lead to both inland and seaward drainage, and favours the rapid downwearing model. These numerical models been complemented by targeted sampling for cosmogenic and thermochronological analysis from the great escarpment of southern Africa in Namibia (Cockburn et al, 2000) and the Drakensberg (Brown et al., 2002). The combination of the new data and the model results implies that this model is more appropriate than a continuous scarp retreat model.

SUMMARY STATEMENT

Overall, the recent advances in our understanding of long term, large scale landscape evolution through uplift and denudation have occurred through new analytical and computational methods, stimulated partly through technological advances, and also through the current research effort focussing on Earth Systems Science. This is motivated by the need to understand the human interaction with the interface of the solid earth and atmosphere, i.e. the Earth's surface. The geological record of the key processes exists, but is often indirect, difficult to decipher and not always obviously linked to modern short term, small scale processes. New and higher resolution dating methods will no doubt emerge to address this issue. Similarly, new computational approaches and carefully

designed field studies will provide insights into the importance and interactions of different processes over a wide range of time and length scales.

REFERENCES

Allen, P. (2005) Striking a chord, Nature, 434, 961.

Arne, D. C. and Zentilli, M. (1994) Apatite fission-track thermochronology integrated with vitrinite reflectance, In : Mukhopadhyay, P.K. and Dow, W.G (Eds) Vitrinite Reflectance as a Maturity Parameter : Applications and Limitations, Am. Chem. Soc. Symposium Series 570, 249-268.

Arne, D.C. , Grist, A.M., Zentilli, M., Collins, M, Embry, A. and Gentzis, T. (2002) Cooling of the Sverdrup Basin during Tertiary basin inversion : implications for hydrocarbon exploration, Basin Research, 14, 183-205.

Beaumont, C. (1981) Foreland Basins, J. Geophys. 65, 291-329.

Beaumont, C., Kooi, H., and Willett, S. (2000) Coupled tectonic-surface process models with applications to rifted margins and collisional orogens, in Geomorphology and Global Tectonics, Summerfield, M.A. (Ed) 29-55., J. Wiley and Sons.,

Bernet, M., Brandon, M.T., Gaver, J.I., Molitor, B.R. (2004) Fundamentals of detrital zircon fission-track analysis for provenance and exhumation studies with examples from the European Alps. In :Bernet, M. and Spiegel, C. (Eds), Detrital Thermochronlogy - Exhumation and Landscape Evolution of Mountain Belts, Geol. Soc. Am. Spec. Pap. 378, 25-36

Bierman, P. R. and Nichols, K.K. (2004) Rock to sediment – Slope to sea with ^{10}Be, rates of landscape change, Ann. Rev. Earth Planet Sci., 32, 215-255.

Braun, J. (2002) Quantifying the effect of recent relief changes on age-elevation relationships, Earth Planet. Sci. Letts., 200, 331-343.

Braun, J. and Beaumont, C. (1989). A physical explanation of the relationship between flank uplifts and the breakup unconformity at rifted continental margins, Geology, 17, 760-764.

Braun, J. and Sambridge, M. (1997) Modelling landscape evolution on geological timescales : a new method based on irregular spatial discretisation, Basin. Res. 9, 25-52.

Brewer, I.D., Burbank, D.W. and Hodges, K.V. (2003) Modelling detrital cooling-age populations : insights from two Himalayan catchments. Basin. Res., 305-320.

Brown RW. (1991) Backstacking apatite fission-track 'stratigraphy' : A method for resolving the erosional and isostatic rebound components of tectonic uplift histories. Geology, 19, 74-77.

Brown, R. W. Summerfield, M. A. and Gleadow, A. J. W. (2002) Denudational history along a transect across the Drakensberg Escarpment of southern Africa derived from apatite fission track thermochronology, J. Geophys. Res. 10.1029/2001JB000745

Brown, R., Gallagher, K., Gleadow, A.J. and Summerfield, M. (2000) Morphotectonic evolution of the South Atlantic margins of Africa and South America, IN, Summerfield, M. (Editor), Geomorphology and Global Tectonics, J. Wiley and Sons, pp. 255-281.

Buck, W.R. (1986) Small-scale convection induced by pssive rifting: the cause for uplift of rift shoulders, Earth Planet. Sci. Letts. 77, 362-372.

Bulat, J. and Stoker, S.J. (1987) Uplift determination from interval velocity studies, : In Brooks, J. and Glennie, K. (Eds), Petroleum Geology of Northwest Europe, Graham and Trotman, London, 293-305.

Burbank, D.W., Blythe, A.E., Putkonen, J., Pratt-Sitaula, B., Gabet, E., Oskin, M., Barros, A. and Ojha, T. P., (2003) Decoupling of erosion and precipitation in the Himalayas, Nature 426, 652–655

Burnham. A.K. and Sweeney, J.J. (1989) A chemical kinetic model of vitrinite reflectance maturation. Geochim. Cosmochim. Acta. 53:2649-2657.

Carlson, W.D. (1990) Mechanisms and kinetics of apatite fission-track annealing. Am Mineral. 75, 1120-1139.

Carson, M.A., and Kirkby, M.J., (1972) Hillslope form and process: Cambridge, UK, Cambridge University Press, 475 pp.

Carter, A. and Moss, S. (1999) Combined detrital-zircon fission-track and U-Pb dating: A new approach to understanding hinterland evolution. Geology. 27, 235-238

Cerling, T.E. and Craig, H. (1994) Geomorphology and in-situ cosmogenic isotopes, Annual Reviews of Earth and Planetary Sciences, 22, 273-317.

Clapp, E.M., Bierman, P.R. and Caffee, M., (2002) Using ^{10}Be and ^{26}Al to determine sediment generation rates and identify sediment source areas in an arid region drainage basin, Geomorphology, 45, 89-104.

Cloetingh, S., McQueen, H. and Lambeck, K. (1985) On a tectonic mechanism for regional sea-level variations, Earth Planet. Sci. Letts. 75, 157-166.

Cochran, J.R. (1983) Effect of finite extension times on the development of sedimentary basins, Earth Planet. Sci. Letts,, 66, 289-302.

Cockburn, H.A.P., Brown, R.W., Summerfield, M.A. and Seidl, M.A. (2000) Quantifying passive margin denudation and landscape development using a combined fission-track thermochronology and cosmogenic isotope analysis approach. Earth Planet. Sci. Letts, 179, 429-435

Dadson, S.J., Hovius, N., Chen, H., Dade, W.B., Hsieh M., Willett, S., Hu, J., Horng, M., Chen, M., Stark, C., Dimitri Lague, D. and Lin, J. (2003) Links between erosion, runoff variability and seismicity in the Taiwan orogen, Nature 426, 648–651.

Davies (1998) Topography : a robust constraint on mantle fluxes, Chemical Geology, 145, 479-489.

Densley, M.R., Hillis, R.R., and Redfearn, J.E.P., (2000) Quantification of Tertiary uplift in the Carnarvon Basin based on interval velocities, Aust. J. Earth Sci., 47, 111-122.

Donelick, R.A., Roden, M.K., Mooers, J.D.,Carpenter, B.S. and Miller, D.S. (1990) Etchable length reduction of induced fission tracks in apatite at room temperature (~23°C): crystallographic orientation effects and “initial” mean lengths. Nucl. Tracks. 17, 261-265.

Dumitru, T.A. (2000) Fission-track Geochronology, In Quaternary Geochronology: Methods and Applications, Stratton Noller, J., Sowers, J.M. and Lettis, W.M. (Eds), AGU reference shelf; 4, 131-156.

Dunai, T. (2000) Scaling factors for production rates of in situ produced cosmogenic nuclides: a critical reevaluation, Earth Planet Sci. Letts. 176, 157-169.

Ehlers, T.A. and Farley, K.A. (2003) Apatite (U-Th)/He thermochronometry: methods and applications to problems in tectonic and surface processes, Earth Planet Sci. Letts ,206, 1-14

England, P. and Molnar, P. (1990) Surface uplift, uplift of rocks, and exhumation of rocks, Geology, 18, 1173-1177.

Farley, K.A. (2000) Helium diffusion from apatite I: General behavior as illustrated by Durango fluorapatite, J. Geophys. Res., 105, 2903-2914 .

Fitzgerald, P.G., Sorkhabi, R.B., Redfield, T.F and Stump, E. (1995) Uplift and denudation of the central Alaska Range; a case study in the use of apatite fission track thermochronology to determine absolute uplift parameters. J. Geophy Res. 100, 20175-20191.

Gallagher, K, dumitru, T and Gleadow, A. (1994) Constraints on the vertical motion of eastern Australia during the Mesozoic, Basin Res., 6, 77-94.

Gallagher, K. (1995) Evolving thermal histories from fission track data, Earth Planet Sci. Letts, 136, 421-435.

Gallagher, K., Brown, R.W. and Johnson, C. J., (1998) Geological Applications of Fission Track Analysis, Annual Reviews of Earth and Planetary Sciences, 26, 519-572.

Garver, J.I, Brandon, M.R, Roden-Rice, M. and Kamp, P.J.J. (1999) Erosional denudation determined by fission-track ages of detrital apatite and zircon, In Ring,U, Brandon, M.T. Willettt, S. and Lister, G. (Eds), Normal Faulting, Ductile Flow and Exhumation Processes, Geol. Soc. Lond. Spec. Publ. 154, 283-304.

Gilchrist, A.R. and Summaerfield, M.A. (1991) Differential denudation and flexural isostasy in the formation of rifted margin upwarps, Nature, 346, 739-742.

Gleadow, A.J.W. and Brown, R.W. (2000) Fission track thermochronology and the long-term denudational response to tectonics In : , IN, Summerfield, M. (Editor), Geomorphology and Global Tectonics, J. Wiley and Sons, pp. 55-75.

Gosse, J.C. and Phillips, F.M. (2001) Terrestrial in situ cosmogenic nuclides : theory and application. Quaternary Science Reviews 20, 1475-1560.

Granger, D.E. Kirchner, J.W. and Finkel, R.C. (1996) Spatially averaged long-term erosion rates measured from in situ-produced cosmogenic nuclides in alluvial sediments, J. Geology. 104, 249-257.

Green, P.F., Duddy, I.R., and Bray, R. (1995) Applications of thernmal history reconstruction in inverted basins, in Buchanan, J.G. and Buchanan, P.G. (Eds) Basin Inversion, Geol. Soc. Lond. Spec. Publ. 88, 148-165.

Green, P.F., Duddy, I.R., and Heggarty, K. A., (2002) Quantifying exhumation from apatite fission-track analysis and vitrinite reflectance datra : precision, accuracy and latest results from the Atlantic margion of NW Europe. In Doré, A.G. Cartwright, J.A., Stoker, M.S., Turner, J.P. and White, N. (Eds), Exhumation of the North Atlantic Margin : timing, Mechanisms, and Implications for Petroleum Exploration. Geol. Soc. Spec. Publ. 196, 331-354.

Green, P.F., Duddy, I.R., Laslett, G.M., Hegarty, K.A., Gleadow, A.J.W. and Lovering, J.F. (1989) Thermal annealing of fission tracks in apatite 4. Quantitative modelling techniques and extension to geological timescales. Chem. Geol. (Isot. Geosci. section). 79,155-182.

Gunnell, Y. (2000) Apatite fission-track thermochronology: an overview of its potential and limitations in geomorphology, Basin Research, 12, 115-132.

Gunnell, Y., Gallagher, K., Carter, A., Widdowson, M. and Hurford, A. J. (2003) Denudation history of the continental margin of western peninsular India since the early Mesozoic – reconciling apatite fission-track data with geomorphology, Earth Planet. Sci. Letts, 215, 187-201

Gurnis, M., Mitrovica, Ritsema,J, and van Heijst, H-J. (2000) Constraining mantle density structure using geological evidence of surface uplift rates : The case of the African Superplume. Geochem, Geophys, Geosys, 1, paper 1999GC000035.

Hillis, R.R. (1995) Regional Tertiary exhumation in and around the United Kingdom, in Buchanan, J.G. and Buchanan, P.G., (Eds), Basin Inversion, Geol. Soc. Lond. Spec. Publ., 88, 167-190.

House, M., Wernicke, B.P. and Farley, K.A. (1998) Dating topography of the Sierra Nevada, California, using (U-Th)/He ages, Nature, 396, 66-69.

House, M.A., Farley, K.A., Kohn, B.P., (1999) An empirical test of helium diffusion in apatite: borehole data from the Otway Basin, Australia, Earth Planet. Sci. Letts,170, 463-474.

Houseman, G. and England, P. (1986) A dynamical model of lithosphere extension and sedimentary basin formation, J. Geophys. Res. 91, 719-729.

Houseman, G., McKenzie, D. and Molnar, P. (1981) Convective instability of a thickening boundary layer and its relevance for the thermal evolution of continental convergent belts, J. Geophys. Res., 86, 6115-6132.

Japsen, P. (1998) Regional velocity-depth anomalies, North Sea Chalk: A record of overpressure and Neogene uplift and erosion, Bull. AAPG, 82, 2031-2074.

Kamp P.J.J., Webster, K.S. and Nathan S. (1996) Thermal history analysis by integrated modelling of apatite fission track and vitrinite reflectance data: Application to an inverted basin (Buller Coalfield, New Zealand) Basin Research, 8, 383-402

Ketcham, R. Donelcik, R. and Carlson, W. (1999) Variability of apatite fission-track annealing kinetics : III. Extrapolation to geological timescales. Am. Mineral. 84, 1235-1255.

Ketcham, R., Donelick, R. and Donelick, M. (2000) AFTSolve : a program for multi-kinetic modelling of apatite fission track data. Geological Materials Research, 2, 1-32.

Kohn, B., Gleadow, A.J.W., Brown, R.W., Gallagher, K., O'Sullivan, P.B. and Foster, D.A. (2002), Shaping the Australian crust over the last 300 million years : insights from fission track thermotectonic imaging and denudation of key terranes, Aust. J. Earth Sciences, 49, 697-717.

Lambeck, K. (1983) Structure and evolution of the intracratonic basins of central Australia, Geophys. J. 74, 843-886.

Lambeck, K. and Nakiboglu, S.M., (1981), Seamount loading and stress in the oceani lithosphere, 2. Viscoelastic and elastic-viscoelastic models. J. Geophys. Res. 86, 6961-6984.

Lambeck, K. and Stpehenson, R.A. (1986) The post-Palaeozoic uplift history of south-eastern Australia, Aust. J. Earth Sciences. 33, 253-270.

Laslett G.M. and Galbraith R. (1996) Statistical modelling of thermal annealing of fission tracks in apatite. Geochim. Cosmochim. Acta 60, 5117-5131

Laslett G.M., Green P.F., Duddy I.R., and Gleadow, A.J.W. (1987) Thermal annealing of fission tracks in apatite 2. A quantitative analysis. Chem. Geol. (Isot. Geosci. section). 65, 1-13.

Lidmar-Bergstrom, K. and Nalsund, J.O. (2002) Landforms and uplift in Scandinavia in Doré, A.G., Cartwright, J.A., Stoker, M.S., Turner, J.P. and White, N. (2002), Exhumation of the North Atlantic Margins : Timing, Mechanisms, and Implications for Petroleum Exploration, Geol. Soc. Lond. Spec. Publ. 196, 103-116.

Lonergan, L. and Mange-Rajetzky, M. (1994) Evidence for internal Zone unroofing from foreland basin sediments, Betic Cordillera, SE Spain, J. geol. Soc. Lond., 151, 515-529.

Mange, M.A. and Maurer, H.F.W. (1992) Heavy minerals in Colour, London: Chapman and Hall

Mayer, L. (2000) Application of digital elevation models to macroscale tectonic geomorphology, in Summerfield, M.A. (Ed) Geomorphology and Global Tectonics, John Wiley and Sons, 15-27.

McKenzie, D. (1978) Some remarks on the development of sedimentary basins, Earth. Planet. Sci. Letts., 40, 25-32.

McKenzie, D. (1984) A possible mechanism for epeirogenic uplift, Nature, 307, 616-618.

Menpes, R.J., and Hillis, R.R., (1995) Quantification of Tertiary exhumation from sonic velocity data, Celtic Sea/South-Western Approaches" In: Buchanan, J.G. and Buchanan, P.G. (eds.) Basin Inversion. Geol. Soc Lond. Spec. Publ., 88, 191-207

Merritts, D. and Ellis, M. (1994) (Eds) Tectonics and Topography, Am. Geophys. Un. Reprinted from J. Geophys Res., Solid Earth v. 99(B6, B7, B10).

Merritts, D. and Ellis, M. (Editors) (1994) Tectonics and Topography, Reprinted from J. Geophys. Res. – Solid Earth, 99 (B6, B7, B10).

Mitrovica, J., Beaumont, C. and Jarvis, G. (1989) Tilting of continental interiors by the dynamical effects of subduction, Tectonics, 8, 1079-1094.

Molnar, P. (2003) Geomorphology: Nature, nurture and landscape, Nature, 426, 612 – 614

Molnar, P. and England, P. (1990) Late Cenozoic uplift of mountain ranges and global climatic change,: chicken or egg ? Nature, 346, 29-34.

Montgomery, D.R. and Brandon, M.T. (2002). Topographic controls on erosion rates in tectonically active mountain ranges. Earth and Planetary Science Letters, 201, 481-489.

Morrow, D. W. and Issler, D.R. (1993) Calculation of vitrinite reflectance from thermal histories: a comparison of some methods; Bull. AAPG, 77, 610-624

Morton, A. C., and Hallsworth, C. R. (1994) Identifying provenance-specific features of detrital heavy mineral assemblages in sandstones. Sed. Geol., 90, 241–256.

Morton, A. C., and Hallsworth, C. R. (1999) Processes controlling the composition of heavy mineral assemblages in sandstones. Sed. Geol., 124, 3–29.

Morton, A.C., Hallsworth, C. and Chalton, B. (2004) Garnet compositions in Scottish and Norwegian basement terrains:a framework for interpretation of North Sea sandstone provenance, Marine Petrol. Geol. 21, 393-410.

Page Chamberlain, C. and Poage, M.A., (2000) Reconstructing the paleotopography of mountain belts from the isotopic composition of authigenic minerals, Geology, 28 115–118.

Partridge, T.C. and Maud, R.R. (1987) Geomorphic evolution of southern Africa since the Mesozoic, S. Afr. J. Geol., 90, 179-208.

Platt, J.P. and England, P.C., (1994) Convective removal of lithosphere beneath moutain belts : thermal and mechanical consequences. Am. J. Sci., 294, 307-336.

Rahl, J.M., Reiners, P.W., Campbell, I.H., Nicolescu, S., and Allen, C.M., (2003) Combined single-grain (U-Th)/He and U/Pb dating of detrital zircons from the Navajo Sandstone, Utah. Geology , 31, 761-764

Reiners, P. W., Ehlers, T. A., Mitchell, S. G. & Montgomery, D. R. (2003) Coupled spatial variations in precipitation and long-term erosion rates across the Washington Cascades, Nature 426, 645–647

Reiners, P.W. and Farley, K.A. (2001) Influence of crystal size on apatite (U-Th)/He thermochronology: an example from the Bighorn Mountains, Wyoming, Earth Planet. Sci. Lett., 188, 413-420

Reiners, P.W., (2002), (U-Th)/He chronometry experiences a renaissance, Eos, v. 83, p. 21-27

Rohrman, M. van der Beek, P.A., van der Hilst, R.J. and Reemst, P. (2002) Timing and mechanisms of North Atlantic uplift : evidence for mantle upwelling.. Landforms and uplift in Scandinavia in Doré, A.G., Cartwright, J.A., Stoker, M.S., Turner, J.P. and White, N. (2002), Exhumation of the North Atlantic Margins : Timing, Mechanisms, and Implications for Petroleum Exploration, Geol. Soc. Lond. Spec. Publ. 196, 27-43.

Rowley, E. and White, N. (1998) Inverse modelling of extension and denudation in the East Irish Sea and surrounding areas, Earth Planet. Sci. Letts, 161, 57-71

Ruddiman, W.F., and Kutzbach, J.E., (1989) Forcing of late Cenozoic Northern Hemisphere climate by plateau uplift in southern Asia and the American West. J. Geophys. Res., v. 94, p. 18409–18427

Sahagian, D.L., and Maus, J.E., (1994) Basalt vesicularity as a measure of atmospheric pressure and paleoelevation: Nature, 372, 449–451.

Sherlock, S.C., Jones, K.A. and Kelley, S.P. (2002) Fingerprinting polyorogenic detritus using the Ar-40/Ar-39 ultraviolet laser microprobe, Geology, 30, 515-518.

Shuster D.L, Vasconcelos ,P.M., Heim J.A., and Farley, K.A. (2005) Weathering geochronology by (U-Th)/He dating of goethite. Geochim, Cosmochim. Acta. 69, 659-673.

Simpson,G. and Schunlegger, F.(2003) Topographic evolution and morphology of surfaces evolving in response to coupled fluvial and hillslope sediment transport. J. Geophys. Res., 108, doi:10,1029/2002JB002162.

Sinclair, H.D. (1997) Flysch to molasse transition in peripheral foreland basins: The role of passive margin versus slab breakoff. Geology, 25, 1123-1126.

Stockli, D.F. Farley, K.A., and Dumitru, T.A. (2000) Calibration of the apatite (U-Th)/He thermochronometer on an exhumed fault block, White Mountains, California, Geology, 28. 983-986.

Stuwe, K. (2002) Geodynamics of the lithosphere : an introduction, Springer-Verlag Berlin, pp. 449.

Summerfield, M. and Cockburn, H. (2004) Geomorphological applications of cosmogenic isotope analysis Prog. Phys. Geog., 28, 1-42

Summerfield, M.A. (2000) Geomorphology and global tectonics : introduction. in Summerfield, M.A. (Ed) Geomorphology and Global Tectonics, John Wiley and Sons, 15-27.

Summerfield, MA. (1991) Global Geomorphology, Longman Scientific & Technical, pp 537.

van der Beek, P. and Braun. J. (1998) Numerical modelling of landscape evolution on geological time-scales : A parameter analysis and comparison with the south-eastern highlands of Australia, Basin Res, 10, 49-68.

van der Beek, P. Summerfield, M. A.; Braun, J.; Brown, R. W. and Fleming, A. (2002) Modeling postbreakup landscape development and denudational history across the southeast African (Drakensberg Escarpment) margin, J. Geophys. Res. 10.1029/2001JB000744

Vasconcelos, P.M. (1999) K-Ar and $^{40}Ar/^{39}Ar$ geochronology of weathering processes

Ventura B., Pini, G.A., Zuffa, G.G. (2001) Thermal history and exhumation of the Northern Apennines (Italy): evidence from combined apatite fission track and vitrinite reflectance data from foreland basin sediments, Basin Research, 13, 435-448.

Vrojlik P, Donelick RA, Queng J, Cloos M. (1992) Testing models of fission track annealing in apatie in a simple thermal setting : site 800, leg 129. In *Proc. Ocean Drilling Program, Scientific Results*. ed. R Larson, Y Lancelot et al. 129:169-176. College Station Texas (Ocean Drilling Program).

Ware, P.D. and Turner, J. P. (2002) Sonic velocity analysis of the Tertiary denudation of the Irish Sea basin, in. In Doré, A.G. et al. (Eds) Exhumation of the North Atlantic Margin : Timing, Mechanisms, and Implications for Petroleum Exploration. Geol Soc. Lond. Spec. Publ. 196, 355-370.

Wheeler, J. and Butler, R. W.H.(1994) Criteria for identifying structures related to true crustal extension in orogens, J. Struct. Geol., 16, 1023-1028

Whipple, K.X. (2001) Fluvial landscape response time : How plausible is steady-state denudation ? Am. J. Sci., 301, 313-325.

Widdowson, M. (1997) Tertiary palaeosurfaces of the SW Deccan, Western India : Implications for passive margin uplift. In Widdowson, M. (ed) Palaeosurfaces: Recognition, Reconstruction, and Palaeoenvironmental Interpretation, Geol. Soc. Lond. Spec. Pub. 120, 221-248.

Willett, S.D (1999) Orogeny and orography the effects of erosion on the structure of mountain belts, J. Geophys. Res., 104, 28957-28981.

Willett, S.D. (1997) Inverse modeling of annealing of fission tracks in apatite 1: A Controlled Random Search method. Am. J. Sci., 297 939-969

Willett, S.D. and Brandon, M.T. (2002) On steady states in mountain belts, Geology, 30, 175-178.

Willett, S.D., Slingerland, R. and Hovius, N. (2001) Uplift, shortening and steady-state topographjy in active mountains belts, Am. J. Sci. 301, 455-485.

Wobus, C. W., Hodges, K. V. & Whipple, K. X. (2003) Has focused denudation sustained active thrusting at the Himalayan topographic front? Geology 31, 861–864.

Wolf, R.A., Farley, K.A. and Silver, L.T. (1996) Helium diffusion and low temperature thermchrononmetry of apatite, Geochim. Cosmochim. Acta, 60, 4231-4240.

Wolfe, J.A., Schorn, H.E., Forest, C.E., and Molnar, P., (1997) Paleobotanical evidence for high altitudes in Nevada during the Miocene: Science, 276, 1672–1675.
Wyllie, M., Gregory, A., and Gardener, L. (1958) Elastic wave velocities in heterogeneous and porous media, Geophysics, 21, 41-70.
Zeitler, P. K. Herczeg, A.L. McDougall, I, and Honda, M. (1987) U-Th-He dating of apatite : A potential geothermometer, Geochim. Cosmochim Acta. 51, 2865-2868.

Isotope	Half-life	Host mineral/rock
^{3}He	Stable	olivine
^{21}Ne	Stable	olivine, quartz
^{10}Be	1.51 x 10^{6} a	quartz
^{26}Al	7.50 x 10^{5} a	quartz
^{36}Cl	3.01 x 10^{5} a	calcite, whole rock

Table 1. Cosmogenic isotopes, their half lives, and common host minerals.

Method	Reference	Location	Problem	Key result
Cosmogenic surface exposure dating	Cockburn et al. (2000)	Namibia	Resolving scarp retreat rate	< 10 m/m.y., incompatible with constant retreat since rifting. Implies a downwearing model.
(U-Th)/He	House et al. (1998)	Sierra Nevada, California	Timing of development of topography	Late Cretaceous, 50-60 m.y. older than thought
AFT	Fitzgerald et al. (1996)	Alaska	Infer denudation and absolute uplift magnitudes	Rock uplift 8.5 km, denudation 5.7 km, mean surface uplift 2.8 km
Vitrinite Reflectance (and AFT)	Green et al. (2002)	Britain and Ireland	Estimate denudation from 2 systems using vertical sections	Infer changes in heat flow and and denudation since the early Cretaceous
Porosity reduction	Japsen (1998)	North Sea Basin	Explain anomalously high and low porosity in Chalk	~ 1km of erosion on margins, overpressure due to low permeability chalk in centre
Burial history	Rowley and White (1998)	East Irish Sea	Estimate missing section	< 1.5 km, generally a minimum relative to AFT/vitrinite reflectance

Table 2. Examples of applications of some of the methods discussed in the text.

FIGURE CAPTIONS

Figure 1.

The relationship between surface uplift (U_s), rock uplift (U_r), and denudation or exhumation (U_e). The geoid is typically approximated by mean sea level.

Figure 2.

The pressure (P_1) associated with thickened continental crust (H_c) compare to the pressure (P_2) in adjacent normal thickness crust (H^0_c). The compensation depth is the depth where these pressures are equal (local isostatic equilbrium) and ρ_c and ρ_m are the densities of the crust and mantle respectively.

Figure 3.

Elevation (in km) associated with crustal thickening (f_c) and lithosphere thickening (f_L). The shaded region is not viable. Redrawn from Stuwe (2002).

Figure 4.

The influence of the necking depth – the shaded band in (a) - on basin and rift flank geometries during extension. If the necking depth is greater than the compensation depth (b), buoyancy forces leading to regional uplift (the flexural response to these forces), while opposite occurs if the necking depth is shallower than the compensation depth (c). Modified from Braun and Beaumont (1989).

Figure 5

(a) Denudation can reduce the mean elevation of a plateau region from $\overline{H}_1$to $\overline{H}_2$ (and crustal thickness), although isostatic rebound can increase local peak heights if deep valley incision occurs (Molnar and England 1990)

(b) Rapid denudation at a scarp front produced during rifting can lead to scarp retreat and the accompanying regional rebound can lead to uplift of the scarp front. The left panel shows the total denudation over 150 Ma, and the total regional rebound in response to this unloading. The scarp front retreats progressively over time, and the elevation of the scarp also increases (after Gilchrist and Summerfield 1991).

Figure 6.

(a) Production of cosmogenic isotopes (in this case ^{10}Be with z* of 60 cm) as a function of depth for 3 times, assuming an initial concentration of zero. The cosmogenic isotopes progressively accumulate at a rate depending on the flux of secondary cosmic rays to a point ($T = \infty$) which represents the steady state between production and decay (relevant to radioactive isotopes).

(b) Concentration of ^{10}Be as a function of time for different erosion rates (E). Faster erosion rates lead to a steady state value more rapidly.

Figure 7.

Predictions of the track length distribution and fission track age for two contrasting thermal histories, shown by the thick line in the top panels. The partial annealing zone is identified by the two dashed lines. The axis on the right of the top panels

refers to the reduced track length (the length normalised by the initial annealed length), and the grey lines show the progressive shortening of 20 tracks formed at successive time increments.

(a) Tracks rapidly shorten to a length in equilibrium with the maximum temperature, which increases with time to the present day value, leading to a symmetrical length distribution, whose mean is indicative of the maximum temperature.

(b) As the temperature decreases, tracks formed more recently experience a lower maximum than the earlier formed tracks and so are longer, leading to a characteristic negatively skewed length distribution

Figure 8.

A summary of the time and depth sensitivity of different dating methods. Cosmogenic surface exposure dating (CSED) is applicable over short length scales (few metres), and timescales up to a few million years (stable isotopes such as ^{3}He and ^{21}Ne may be extended to longer timescales). (U-Th)/He and AFT are generally applicable to longer timescales, and as a consequence of their respective temperature sensitivities are applicable to depth ranges between 1-4 km. (U-Th)/He is sensitive to lower temperatures than AFT, but the temperature ranges overlap (thanks to Roderick Brown for this figure).

Figure 9.

The temperature and time dependence of vitrinite reflectance compared with AFT. The grey lines are vitrinite reflectance (Ro%), and the dashed lines are mean track length (μm). The point of total annealing is marked by the thick line, corresponding to about 0.7 Ro%. The 2 systems behave similarly, but vitrinite reflectance can be extended to higher temperatures and is a useful maximum temperature indicator. However, fission track data provide additional information about the post-maximum temperature thermal history (see figure 6).

Figure 10.

The principles behind estimating denudation, or missing section, using porosity. The reference porosity-depth function (solid curve) is determined from porosity (or sonic velocity) data in regions with no denudation. The open circles represent porosity data which are anomalously low for the present depth. Denudation is estimated by the offset of the mean depth from the reference curve.

Figure 11.

The principles behind the use of subsidence curves in extensional basins to estimate denudation. After backstripping, the tectonic subsidence curve is used to infer the extension history, separated into the syn-rift and post-rift thermal subsidence components. It is possible then to predict the expected subsidence, up to the present day, and denudation is estimated from the difference between the prediction and the observed subsidence.

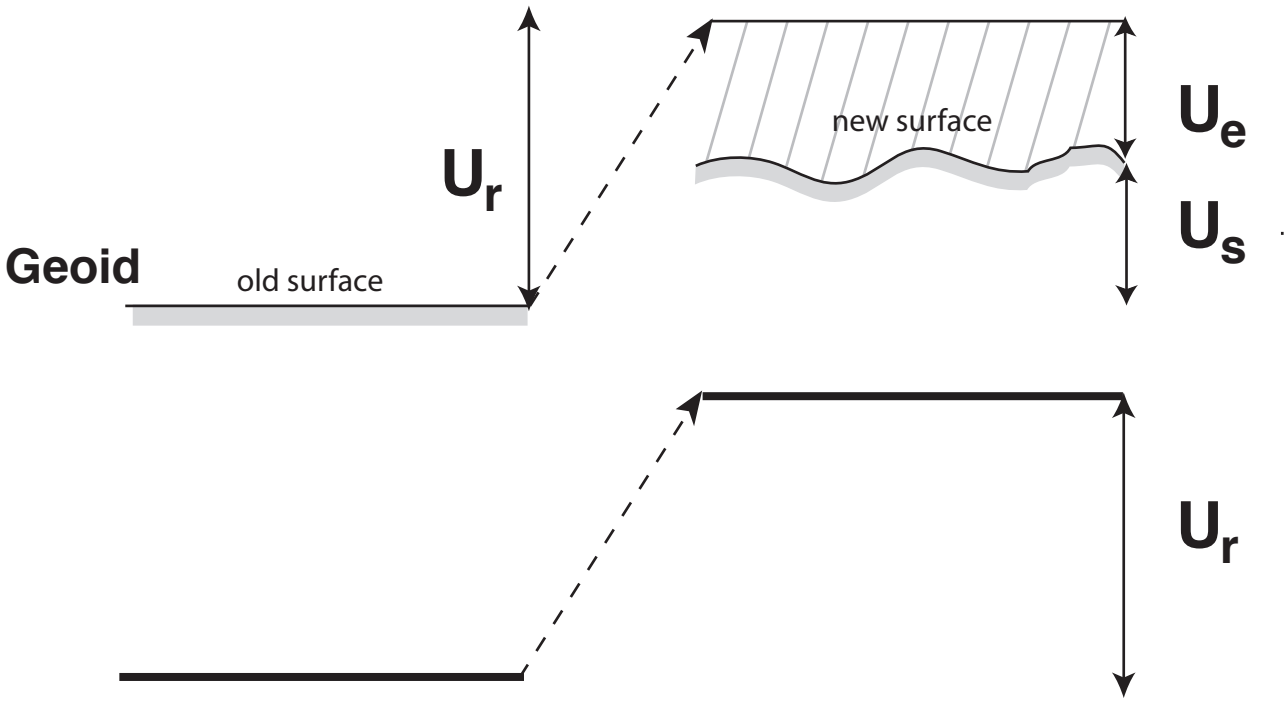

Gallagher : Figure 1

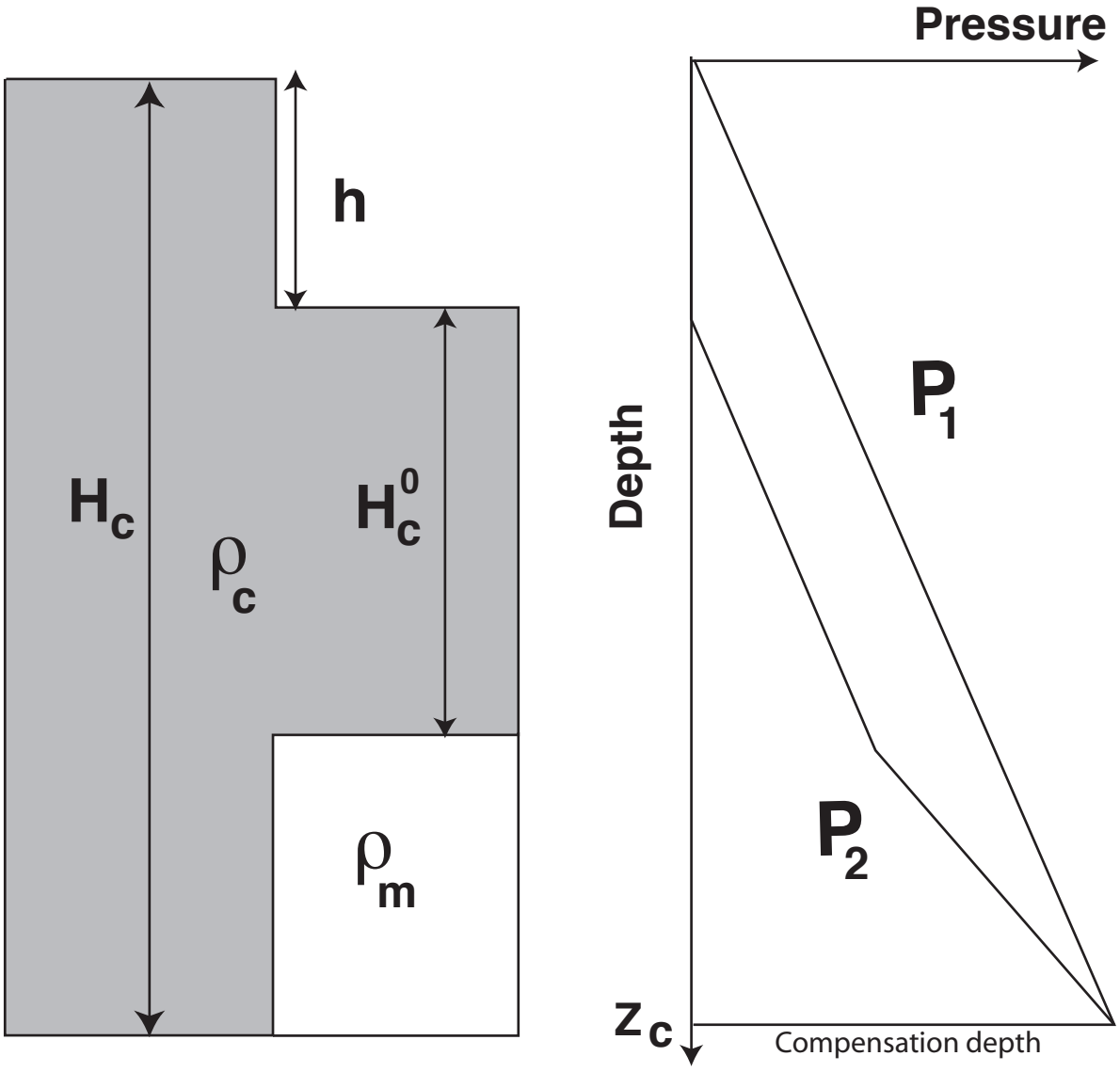

Gallagher : Figure 2

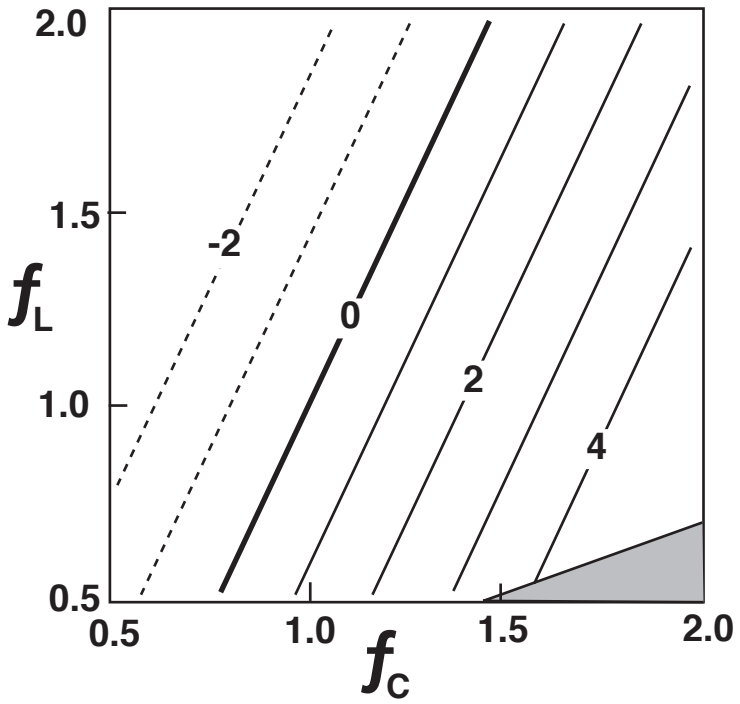

Gallagher : Figure 3

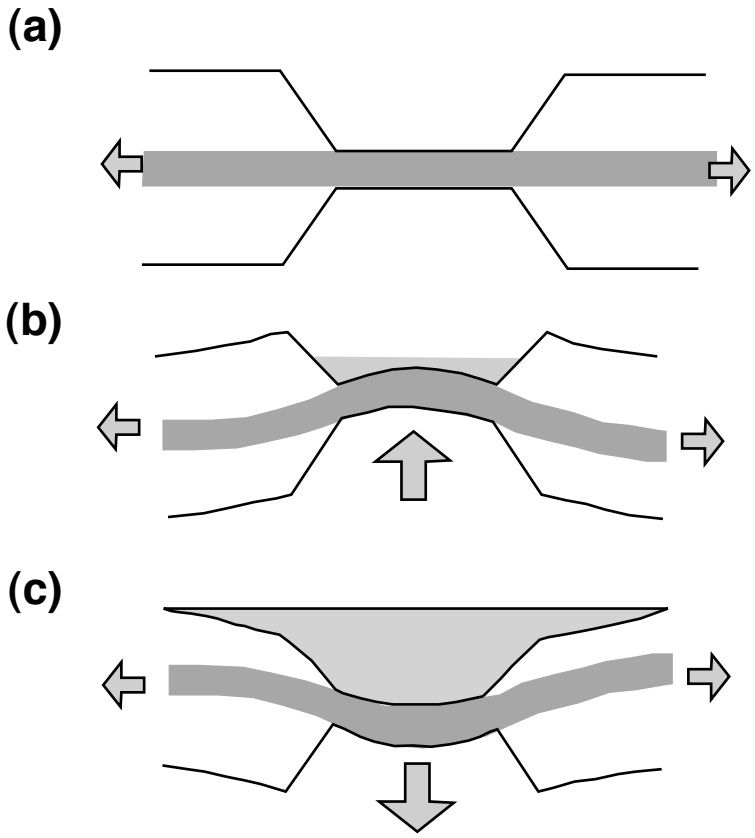

Gallagher : Figure 4

(a) Local isostasy

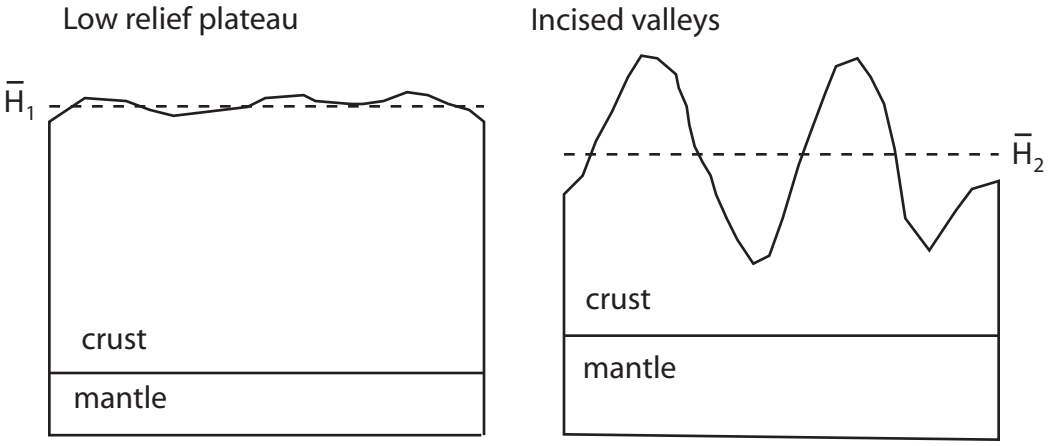

(b) Flexural isostasy

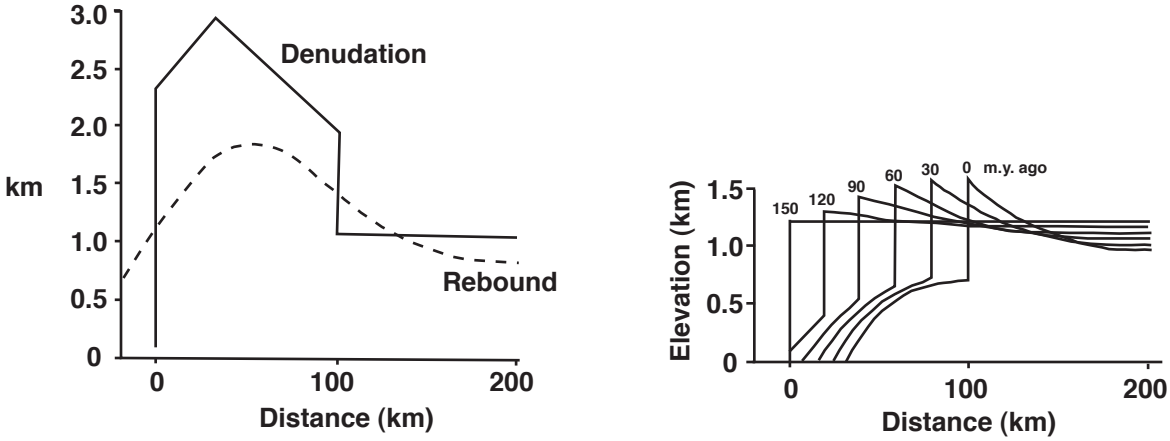

Gallagher : Figure 5

(a)

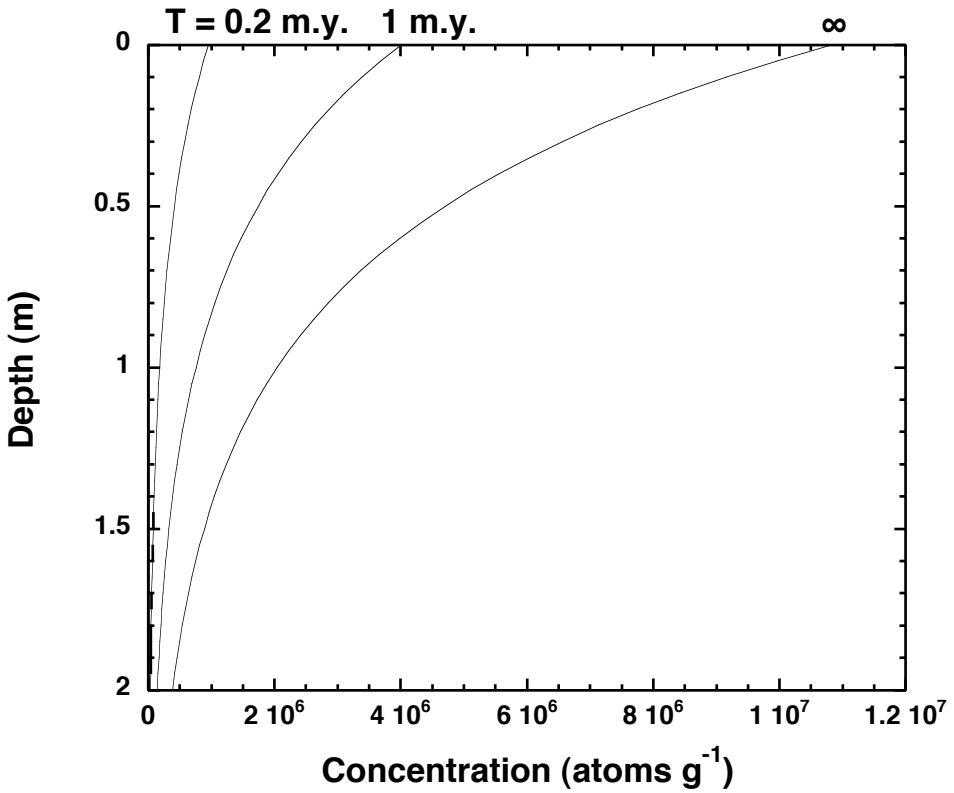

(b)

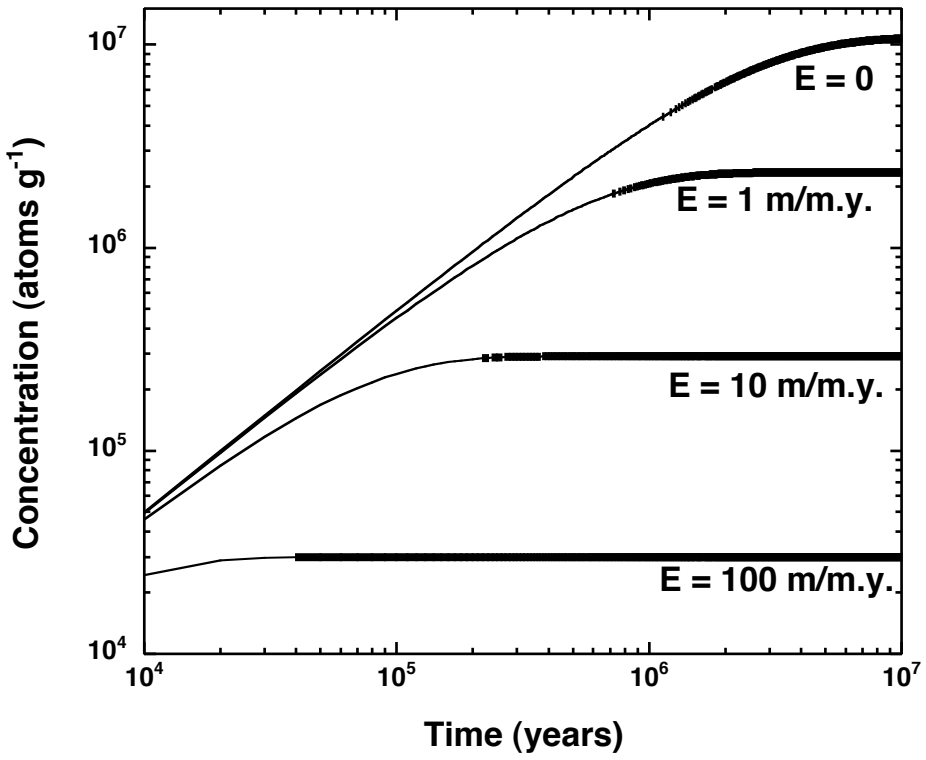

Gallagher : Figure 6

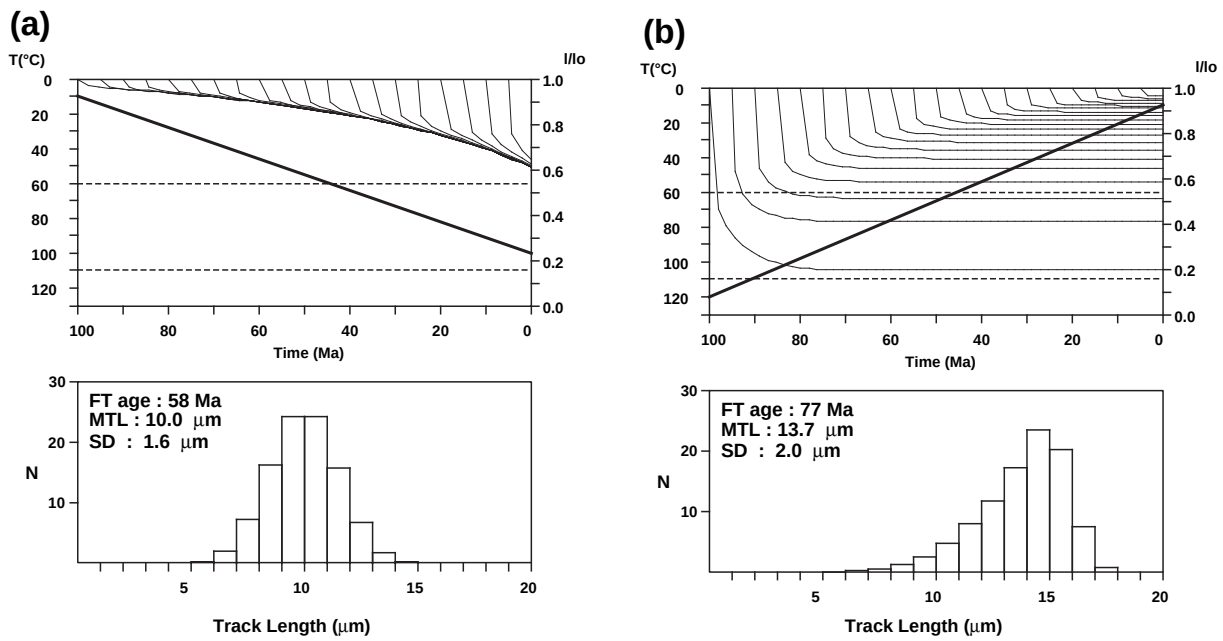

Gallagher : Figure 7

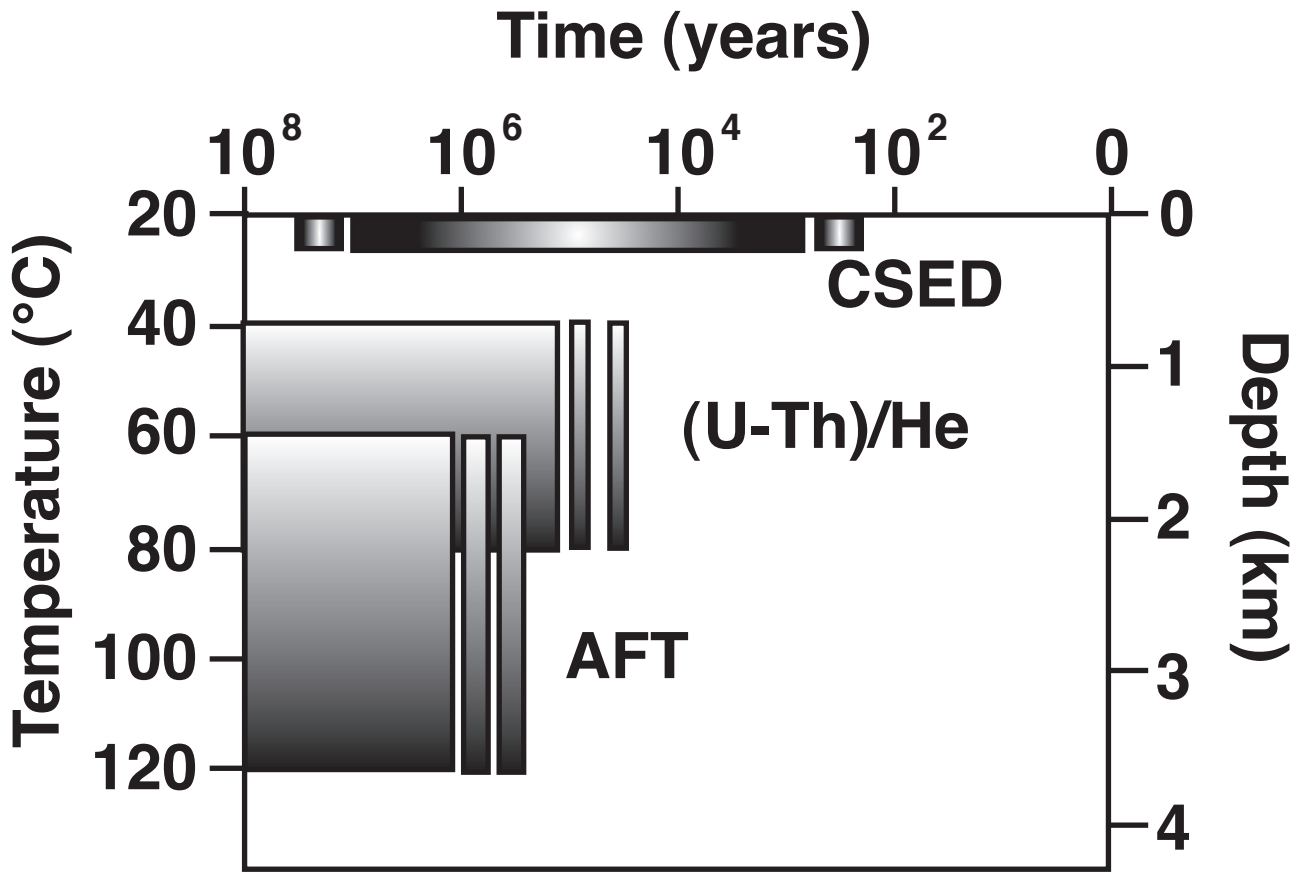

Gallagher : Figure 8

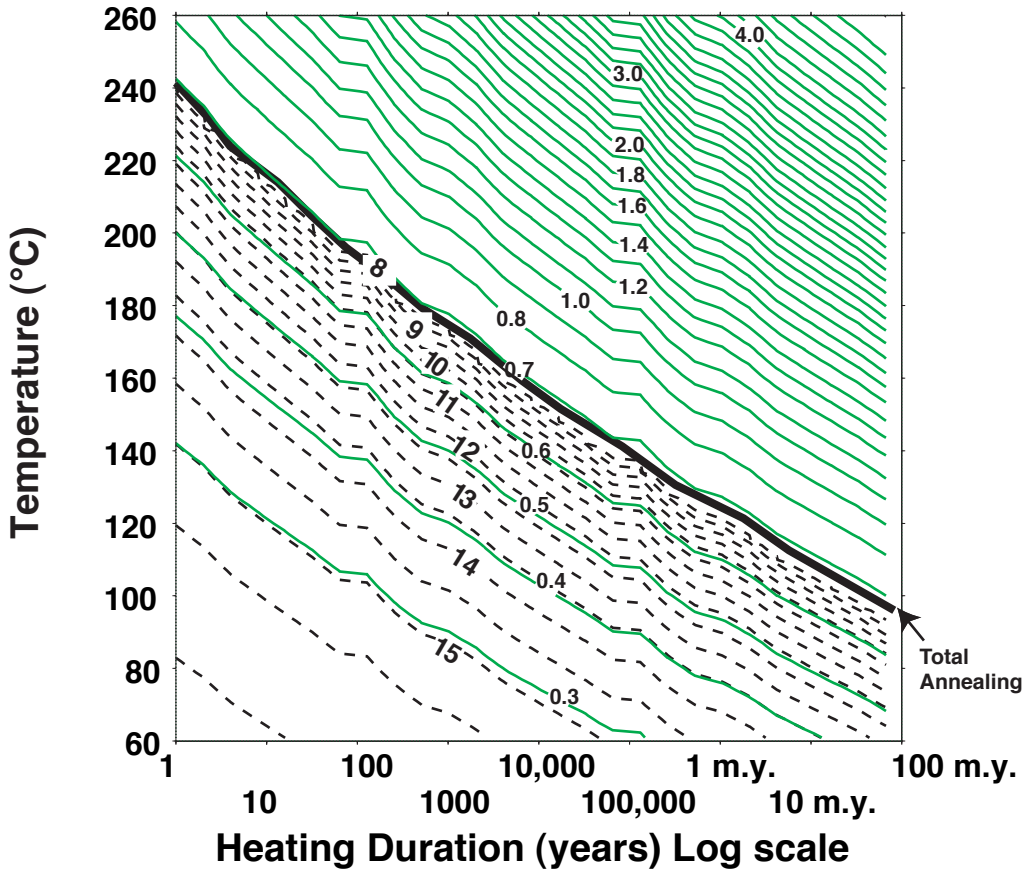

Gallagher : Figure 9

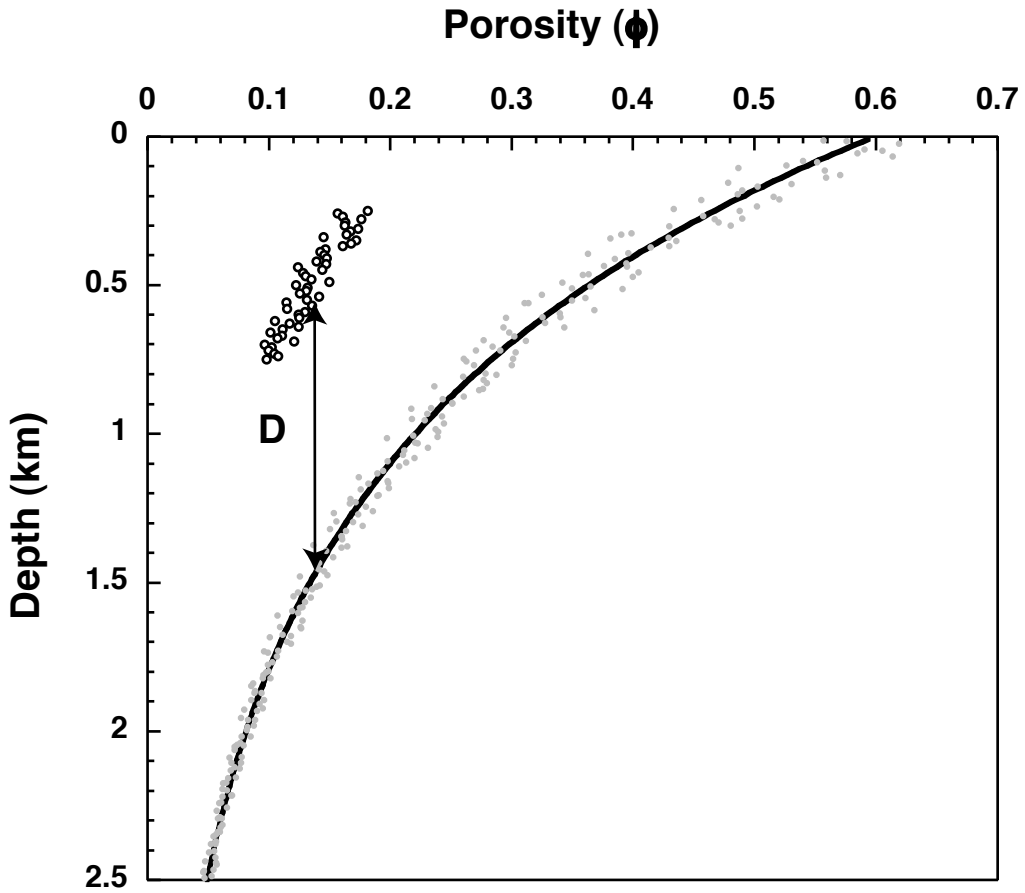

Gallagher : Figure 10

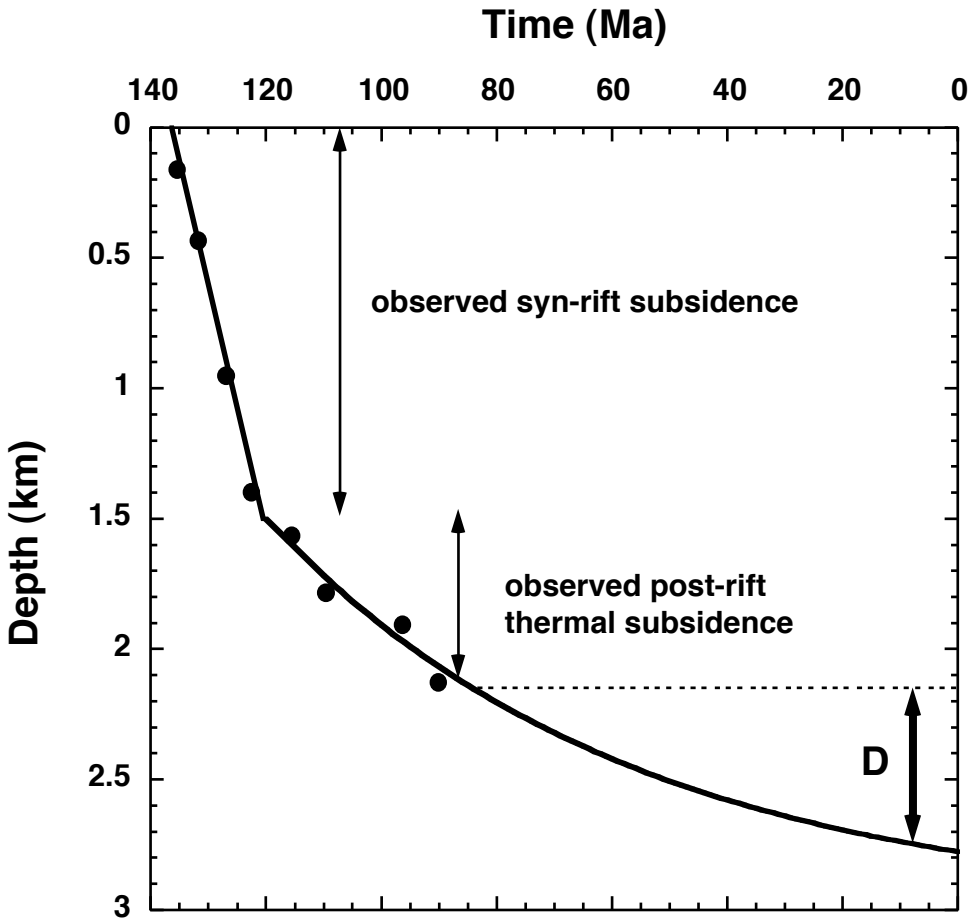

Gallagher : Figure 11